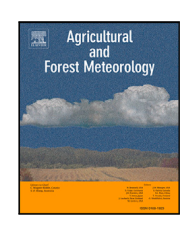
\$ 50 CONTRACTOR OF THE SECOND SECOND

Contents lists available at ScienceDirect

Agricultural and Forest Meteorology

journal homepage: www.elsevier.com/locate/agrformet





A Bayesian inference approach to determine experimental *Typha latifolia* paludiculture greenhouse gas exchange measured with eddy covariance

Alexander J.V. Buzacott ^{a,*}, Merit van den Berg ^a, Bart Kruijt ^b, Jeroen Pijlman ^c, Christian Fritz ^d, Pascal Wintjen ^e, Ype van der Velde ^a

- ^a Earth and Climate, Vrije Universiteit Amsterdam, De Boelelaan 1105, Amsterdam, 1081 HV, Netherlands
- b Water Systems and Global Change Group, Wageningen University and Research, Droevendaalsesteeg 4, Wageningen, 6708 PB, Netherlands
- ^c Louis Bolk Institute, Kosterijland 3-5, Bunnik, 3981 AJ, Netherlands
- d Aquatic Ecology and Environmental Biology, Institute for Water and Wetland Research, Radboud University, Houtlaan 4, Nijmegen, 6525 XZ, Netherlands
- e Netherlands Organisation for Applied Scientific Research (TNO), Westerduinweg 3, Petten, 1755 ZG, Netherlands

ARTICLE INFO

Dataset link: https://github.com/buzacott/Zeg veldBayesianFluxes

Keywords: Peat Carbon dioxide Methane Flux footprint Annual totals

ABSTRACT

Measurements of greenhouse gas exchange (GHG) using the eddy covariance method are crucial for identifying strategies to achieve emission reductions and carbon sequestration. There are many sites that have heterogeneous land covers where it would be useful to have balances of particular land areas, such as field trials of emission mitigation strategies, but the flux footprint infrequently covers only the area of interest. Filtering the data based on a footprint area threshold can be done but may result in the loss of a high proportion of observations that contain valuable information. Here, we present a study that uses a single eddy covariance tower on the border of two land uses to compare GHG exchange from a Typha latifolia paludiculture experiment and the surrounding area (SA) which is primarily a dairy meadow. We used a Bayesian inference approach to predict carbon dioxide (CO₂) and methane (CH₄) fluxes where the relative contribution of the two source areas, derived from a two-dimensional footprint for each timestep, was used to weight and parameterise equations. Distinct differences in flux behaviour were observed when contributions of the two land areas changed and that resulted in clearly different parameter distributions. The annual totals (posterior mean \pm 95% confidence interval) from the simulations showed that Typha was a net sink of CO₂ for both simulation years (-18.5 \pm 2.9 and $-17.8 \pm 2.9 \text{ t CO}_2 \text{ ha}^{-1} \text{ yr}^{-1}$) while SA was a net source (16.8 \pm 2.9 and 17.4 \pm 2.9 t CO₂ ha⁻¹ yr⁻¹). Using the 100-year global warming potential of CH₄, even though CH₄ emissions were higher for paludiculture in both years $(13.6 \pm 0.6 \text{ and } 15.9 \pm 1.0 \text{ t CO}_2\text{-eq ha}^{-1} \text{ yr}^{-1})$ than SA $(7.1 \pm 0.6 \text{ and } 6.8 \pm 1.2 \text{ t CO}_2\text{-eq ha}^{-1} \text{ yr}^{-1})$, the net GHG balance indicates that Typha paludiculture is a viable strategy to limit GHG emissions from drained peatlands.

1. Introduction

Eddy covariance (EC) is a direct method to measure turbulent fluxes of energy, gases and momentum between the biosphere and atmosphere (Mauder et al., 2021). The development of EC has been crucial to improve our understanding of terrestrial and atmospheric functioning over the past 30 years (Baldocchi, 2020). There are many sites where it is desirable to observe the exchange of GHGs but they may not be ideal places to measure with EC. Homogeneity of the flux source area is an assumption of the EC method, however heterogeneity is frequently a reality. This is often the case in natural and disturbed peatland ecosystems, where there can be a mix of vegetation, and presence of drainage ditches or water bodies that can have drastically different carbon source

and sink behaviour. Field experiments are another example, where it may be desirable to assess the effect of a treatment *in-situ* and at the same moment in time, rather than applying treatments in time or having to use multiple sets of equipment in space, which is especially costly for trace gases such as methane ($\rm CH_4$) or nitrous oxide ($\rm N_2O$) (Goodrich et al., 2021). Alternative measuring methods exist that could be deployed in such situations such as static or automatic chambers, but they have their own deficiency of being point scale measurements that disturb the measuring point (Riederer et al., 2014; Poyda et al., 2017). EC is ideal in that it can provide ecosystem-scale measurements over long time periods with minimal disturbance to the environment and relatively low maintenance requirements (Baldocchi, 2003).

E-mail addresses: a.j.v.buzacott@vu.nl (A.J.V. Buzacott), m.vandenberg@vu.nl (M. van den Berg), bart.kruijt@wur.nl (B. Kruijt), j.pijlman@louisbolk.nl (J. Pijlman), christian.fritz@ru.nl (C. Fritz), pascal.wintjen@tno.nl (P. Wintjen), ype.vander.velde@vu.nl (Y. van der Velde).

^{*} Corresponding author.

Studying different source areas of interest can be achieved with footprint models (Vesala et al., 2008; Leclerc and Foken, 2014). For each moment in time, the source area of the flux can be estimated and then the flux can be attributed to different land features (Wang et al., 2006; Franz et al., 2016; Tuovinen et al., 2019; Chu et al., 2021; Rey-Sanchez et al., 2022), providing a more precise comparison of different land elements than by partitioning based simply on wind direction. Unwanted land features can also be excluded more precisely. Fast two-dimensional footprint prediction models, such as the models of Kormann and Meixner (2001) and Kljun et al. (2015), drastically reduce the computation time required and it is feasible to obtain footprints for each timestep for multiple years compared to sophisticated Lagrangian stochastic particle dispersion models (e.g., Kljun et al., 2002).

A timeseries of fluxes from a specific part of the footprint can be obtained by spatially analysing each footprint and retaining only the timesteps where some minimum threshold (e.g., 50%, 70%) was estimated to come from the desired area (Chu et al., 2021). This can cause many timepoints to be marked as missing and subsequently need to be gapfilled for annual budget estimates. If a lower threshold is used, this also means that the flux source is mixed for many timesteps and less representative of the desired area. Some studies have also compared fluxes from adjacent fields using a single EC system. Fuchs et al. (2018) and Goodrich et al. (2021) compared adjacent fields to study emission mitigation options of N2O fluxes, and Wall et al. (2020) examined carbon dioxide (CO2) fluxes from adjacent fields. These studies also used contribution thresholds to define the source areas. For example, Wall et al. (2020) used a contribution threshold of 70% during the day and 60% at night, with the latter lower value to compensate for the lower number of observations at night due to low turbulence. In these studies, after the different timeseries were defined by using the footprint thresholds, they were gapfilled independently. However, all timesteps with a mixed contribution from different land features contain information about all these land features, and a method that uses this valuable information is wanted.

A special case of where large differences in emission behaviour in a landscape can be found is in peatland rewetting and rewetting strategy trials. Peatlands are an important storage of carbon (C) and contain more than 30% of the Earth's soil C (Lamers et al., 2015), despite only covering approximately 3% of the global surface area (Yu et al., 2010). The formation of peat occurs in areas with high rainfall or poor drainage where the soil saturates, limiting the supply of oxygen and inhibiting decomposition of organic matter. Many peatlands have been drained for productive agricultural and forestry use. While natural peatlands may be net annual C sinks (Nilsson et al., 2008; Dinsmore et al., 2010; Koehler et al., 2011), drainage enables microbial peat oxidation that increases CO₂ emissions (Renou-Wilson et al., 2014; Wilson et al., 2015; Prananto et al., 2020) and causes land subsidence (Erkens et al., 2016). The drainage and disturbance of peatlands poses a large risk to the climate, given their large and relatively vulnerable C pool that can readily exchange with the atmosphere (Frolking et al., 2011). Drained peatlands cover 0.3% of the Earth's surface area but are responsible for around 5% of the global anthropogenic CO2 emissions (Joosten et al., 2016) and reducing emissions from drained peatlands is required to limit global warming (Leifeld et al., 2019).

The rewetting of drained peatlands is a relatively easy strategy to reduce C emissions or sequester C (Wilson et al., 2016; Leifeld and Menichetti, 2018) with moderate expenses (Bonn et al., 2016). Evidence generally points to rewetting having a neutral to cooling effect on the climate (Kivimäki et al., 2008; Waddington et al., 2010; Schwieger et al., 2021), despite the increase in CH₄ emissions (Günther et al., 2020; Evans et al., 2021). Paludiculture is often proposed as a rewetting option to mitigate emissions while keeping productive land Geurts et al. (2019), de Jong et al. (2021). Paludiculture is the practice to cultivate crops on wet conditions or shallow water tables (Joosten et al., 2012). So-called paludicrops that are often established are tall helophytes, namely *Phragmites australis* (reeds) and *Typha spp*.

(cattail). In north-western Europe, reeds are widely established, while cattail species are still in pilot or experimental settings. Cattail in particular is a promising paludicrop as the physical characteristics of the crop make it suitable material for insulation (Luamkanchanaphan et al., 2012; Georgiev et al., 2013; Krus et al., 2015; de Jong et al., 2021). As the type of vegetation on peat can influence the emissions of CH₄ (Hendriks et al., 2010; Bhullar et al., 2014; van den Berg et al., 2016, 2020), paludicrops that also suppress CH₄ emissions are ideal. A concern about Typha spp, such as Typha latifolia as (broadleaf cattail) and Typha angustifolia (narrowleaf cattail), is the potential for high CH4 emissions due to its efficient internal gas transport mechanism (Bendix et al., 1994; Vroom et al., 2022). However, due to the various factors that influence emissions from rewetted peatlands, such as from substrate and nutrient availability, there may be substantial variability in emissions (IPCC, 2014; Wilson et al., 2016). There is a clear need for more studies on the GHG exchange from paludiculture trials. However, the size of the field trials, and more generally just fields in the Netherlands, is often problematic for EC, where the footprint may not cover the desired source area all the time. Additionally, it would be desirable to compare the fluxes from adjacent fields as a comparison to see if the GHG exchange behaviour is different and that mitigation strategies are effective.

In this study, we aim to develop a method to exploit the information contained in timesteps with mixed source area contributions measured by a single EC tower, rather than discard them. We use the flux footprint and empirical CO_2 and CH_4 prediction models to constrain the flux source behaviour and test it on a two-year timeseries from a mixed paludiculture-meadow field site in the Netherlands. Specifically, our aims were to: (1) develop a Bayesian inference approach that can identify probable parameter sets for models that predict CO_2 and CH_4 fluxes for multiple land elements in a heterogeneous field site, (2) demonstrate the skill and advantages of our approach compared to standard flux filtering and gapfilling approaches, and (3) compare and evaluate the annual emissions of the paludiculture trial to the adjacent field.

2. Materials and methods

2.1. Study site

Fluxes of CO2 and CH4 were measured at a field site on the experimental farm KTC Zegveld (52.14N, 4.84E, -2.3 m elev), located in the west of the Netherlands between May 2020 and December 2022 (Fig. 1). The climate is temperate and humid, with a mean annual temperature and precipitation of 10.5 \pm 0.7 °C and 766 \pm 141 mm, respectively, for the period 1991 to 2020 (Cabauw, KNMI ID: 348). The peat soils at Zegveld have a clay rich topsoil that overlays 6 to 7 m of wood sedge peat Langeveld et al. (1997). The typical land use of Zegveld is intensive grazing by dairy cattle and the vegetation is dominated by Lollium perenne (perennial ryegrass) and Poa pratensis (meadow grass). A 0.4 ha parcel of Typha latifolia (common name cattail, henceforth simply Typha) was established in July 2016 as a paludiculture experiment. Prior to establishment, approximately 10 to 20 cm of the topsoil was excavated and was used to create a small dike around the parcel edge to ensure that the Typha had a standing water level above the ground surface. More details about the establishment of the field are provided in Pijlman et al. (2019). In the first year of field establishment, 2016, no fertiliser was applied to the Typha field, but from 2017 to 2020 nutrients were added. In 2017 and 2018 150 kgN ha⁻¹ as coated urea and 150 kgK ha⁻¹ as coated potassium nitrate (Ekompany, Born, Netherlands) were applied. The same amount of nutrients was used in 2019 and 2020 but were in the form of ammonium nitrate, potassium chloride, and monocalcium phosphate. In 2021 and 2022, no nutrients were added. There was an annual Typha harvest usually between February and March. The Typha here grow to an average height of around 2 m.

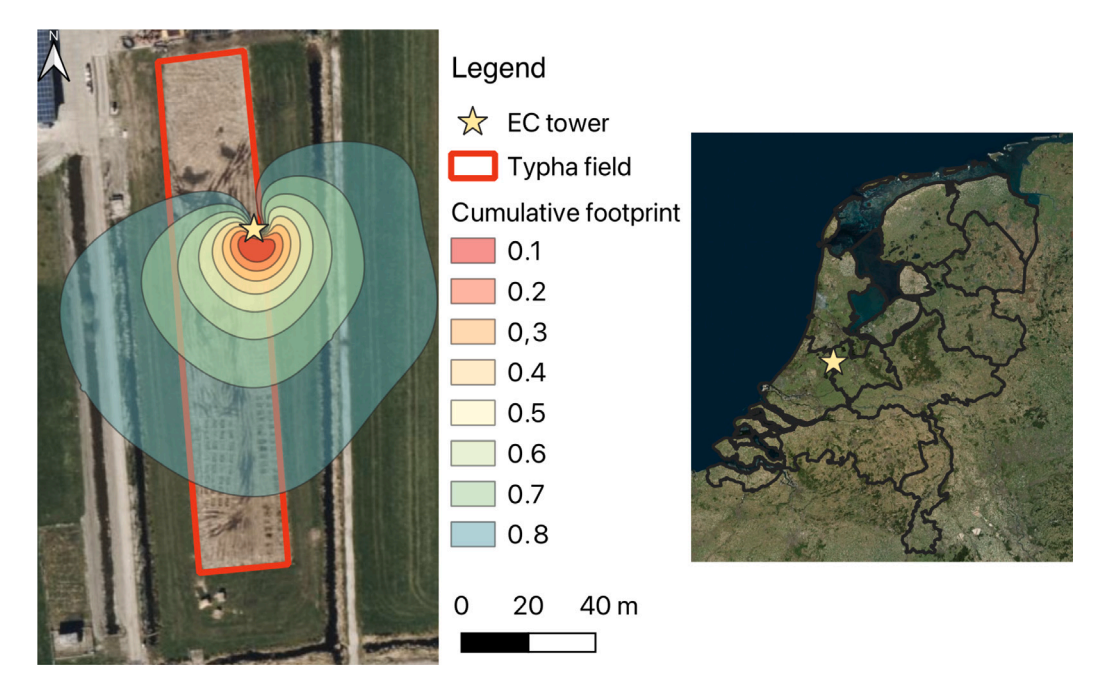


Fig. 1. The location of the study site in the Netherlands (right) and an overview of the Zegveld field site (left). The footprint contours were calculated using the mean footprint over the study period, where the footprints were estimated with the Kljun et al. (2015) model. Timesteps where the wind direction was lower than 60 degrees or more than 265 degrees were excluded to avoid built-up farm area.

2.2. Measurements and ancillary data

An EC system was setup in the north eastern corner of the *Typha* field (Fig. 1). The predominant wind direction is from the southwest, and hence the location of the EC system was set to mainly capture fluxes from the *Typha* field. A Metek uSonic-3 Cage MP sonic anemometer (Metek GmbH, Elmshorn, Germany) was used to record three-dimensional wind speed and heat fluxes. Open path gas analysers for $\rm CO_2$ and $\rm H_2O$ (LI-7500DS, LI-COR Biosciences, Lincoln NE, USA) and $\rm CH_4$ (LI-7700, LI-COR Biosciences, Lincoln NE, USA) were used to measure gas concentrations. Raw data were recorded at a 10 Hz frequency by a Smartflux 3 system (LI-COR Biosciences, Lincoln NE, USA), which uploaded the data to a central database via telemetry. The height of the EC system was fixed at 3 m above the ground, meaning that the height above the maximum vegetation was 1 m for *Typha* and 2.5 m for the pasture. The data used in this study was collected between February 2021 and December 2022.

A meteorological station was installed next to the EC system. Short and longwave radiation components were measured using an Apogee SN500SS net radiometer (Apogee Instruments, North Logan, Utah, USA), air temperature and humidity with a Campbell HygroVUE5 (Campbell Scientific, Utah, USA), soil temperature at 10 and 30 cm depth with a Campbell 107 probe, and water level with a Campbell CS450 pressure transducer. Raw data were recorded using a Campbell CR1000X data logger, which was connected to the Smartflux 3 system. A separate weather station located approximately 300 m to the southeast of the EC tower was also used. This station consisted of a Gill Maximet GMX500 system that measured air temperature, relative humidity, atmospheric pressure, precipitation, wind speed and direction was combined with an Apogee SN500SS net radiometer and a Skye SKR1840 two channel light sensor (Skye Instruments, Powys, UK) to measure photosynthetically active radiation (PAR). All meteorological data were recorded at a one-minute frequency and then averaged into 30-min records.

Meteorological data from the nearest Royal Netherlands Meteorological Institute (KNMI) weather station approximately 20 km east of the study site (Cabauw location A (KNMI ID: 348)) were retrieved in case meteorological records required gapfilling. Records of temperature

and humidity, atmospheric pressure, wind speed direction, global radiation, and precipitation were obtained from the KNMI data platform (https://dataplatform.knmi.nl). The data retrieved were 10-min records and were aggregated into 30-min records.

2.3. Flux calculation

Turbulent fluxes were calculated using the covariance of vertical wind speed and scalars of interest using EddyPro (v7.0.9, LI-COR Biosciences). The flux averaging interval was 30-min and the missing sample allowance was 10%. Raw data were screened using the (Vickers and Mahrt, 1997) tests for spike removal, amplitude resolution, drop-outs, absolute limits, skewness and kurtosis, and discontinuities. Corrections were applied to the covariances, including double coordinate rotation for tilt correction, block averaging for detrending, covariance maximisation for time lag detection, and compensation for density fluctuations for the open path systems (Webb et al., 1980). Compensation for spectroscopic effects of temperature, pressure, and water vapour were also applied for the LI-7700 (McDermitt et al., 2011; Burba et al., 2019). Fully analytic low frequency (Moncrieff et al., 2004) and high frequency (Moncrieff et al., 1997) spectral corrections were applied. The net ecosystem exchange (NEE) for each scalar was calculated as the turbulent flux plus the single point storage estimate for each timestep (Aubinet et al., 1999). Dynamic metadata for canopy height of the Typha was used as input for the flux calculation that was based on observations or interpolated estimates at a one-week frequency. Potential impacts of this on the footprint modelling are discussed later.

The 30-min fluxes were postprocessed using a series of filters. CO_2 and CH_4 fluxes were filtered according to the Mauder and Foken (2004) 0–1–2 system, where only fluxes with a flag of 0 (indicative of the highest quality) were selected for further analysis. A received signal strength indicator (RSSI) threshold of 70 was used for the CO_2 fluxes and a threshold of 10 for CH_4 . The CH_4 threshold of 10 was chosen as it indicates when the sample path is blocked or the mirrors have been fouled (McDermitt et al., 2011). Flux values for CH_4 between -0.05 to $2 \, \mu \text{mol} \, \text{m}^{-2} \, \text{s}^{-1}$ were considered realistic, and values outside that range were marked as missing. To remove poorly turbulent conditions that

occur at night, a friction velocity (u*) threshold was determined using the moving point test (Papale et al., 2006). The u* threshold determined by the algorithm was $0.06\,\mathrm{m\,s^{-1}}$, and night-time fluxes below this threshold were marked as missing. Fluxes were only accepted between the wind directions 60 and 265 degrees to avoid built-up farm area to the north of the EC instrument. After filtering, 25% of the CO₂ and 17% of CH₄ flux timesteps remained for analysis.

2.4. Footprint modelling

The (Kljun et al., 2015) two-dimensional fast footprint prediction (FFP) model was used to estimate the flux footprint for each 30-min timestep. The model requires input that is readily sourced from the EC tower and field observations, including the measurement above displacement height, roughness length, mean wind speed, wind direction, Monin-Obukhov length, and the standard deviation of lateral wind velocity fluctuations. Temporal changes in the zero-plane displacement height and roughness length were determined based on a mixture of observations and expected canopy growth over time. We used standard approximations for the zero-plane displacement height and roughness length of 0.67 and 0.15 multiplied by the canopy height, respectively. The last model input required is the planetary boundary layer height (PBLH). We followed the recommendation of Kljun et al. (2015, Appendix B) and used estimates of the PBLH from a Lufft CHM 15k ceilometer (OTT HydroMet Fellbach GmbH, Fellbach, Germany) from the KNMI site Cabauw (KNMI ID: 06348), also obtained from the KNMI data portal. The ceilometer detects aerosols in the atmosphere and the lowest aerosol layer that can be detected can be interpreted as the PBLH. The ceilometer records data at a 12 s frequency and comes with an associated quality flag from 0 to 9. After inspection of the quality flags and data, all data with a flag of 5 and higher was marked as missing and the data was averaged into 30-min intervals to match the frequency of the flux data.

All footprints were calculated with the R adaptation of Kljun et al. (2015) FFP model code that was retrieved from https://footprint.kljun. net. The size of the footprint calculation area was $\pm 240\,\mathrm{m}$ for the x,y axes from the EC tower and the resolution was $1\times 1\,\mathrm{m}$. Every valid footprint for a 30-min timestep was rasterised and the weighted contribution of the flux originating from the Typha field was extracted and summed. The sum of the proportion of the flux originating from inside the Typha field was divided by the total to estimate the contribution percentage and is henceforth referred to as CB_{Typha} . The estimate of the surrounding area (SA) outside the Typha plot, CB_{SA} , is then simply calculated as $CB_{SA} = 1 - CB_{Typha}$.

A valid footprint could not be estimated for every timestep for a variety of reasons, such as when the friction velocity was too low or when power failures resulted in no EC data being recorded. To replace missing timesteps where the contribution of the *Typha* field to the flux could not be estimated, a Random Forest (Breiman, 2001) model was used. The model was trained with inputs of wind speed, wind direction, and day of the year to predict the percentage of the flux originating from the *Typha* field. The model was trained with a random sample of 70% of the data and tested with 30%. The model achieved a Lin's concordance correlation coefficient (LCCC) of 0.99 in the training round and 0.98 in the testing round. The gapfilled contributions were only used for the timeseries of the simulated EC tower (i.e., combination of the flux sources) and not for the individual sources, and, most importantly, not for model parameter identification or annual budgets of the individual sources.

2.5. Bayesian inference and flux modelling

The partitioning and inference of NEE into ecosystem respiration ($R_{\rm eco}$) and gross primary production (GPP), modelling of CH₄ flux (FCH₄), as well as mixing of the flux sources, was performed in a Bayesian framework. The general Bayesian framework is described first,

followed by the gas specific equations used to model the fluxes. Relative posterior probabilities are assigned to model parameters θ given the observed data d according to Bayes' theorem:

$$P(\theta|d) \propto P(d|\theta)P(\theta)$$
 (1)

where the prior $P(\theta)$ is an informed or uninformed probability distribution about the model parameters θ before considering the observed data d, and the likelihood $P(\mathbf{d}|\theta)$ is the probability distribution of d given θ . A Markov Chain Monte Carlo (MCMC) with the Differential-Evolution (DEzs) sampling algorithm (ter Braak and Vrugt, 2008) was used via the R package BayesianTools (Hartig et al., 2019).

We used two model rounds: firstly, to define a probable parameter space for each land use and secondly to use all timesteps with mixed contribution. For the first-round, data was subset using 70% thresholds of CB_{Typha} and CB_{SA} to define fluxes originating from inside the Typha plot and outside. The decision to use 70% flux source contributions corresponding to inside and outside the Typha plot was motivated by the idea to yield parameter distributions that reasonably resemble the two flux sources considering the distribution of available data, and it is the minimum percentage recommended by Mauder et al. (2013). Uniform prior distributions were used for all parameters in the first-round and their ranges are presented in Table A.1. In the following equations, NEE is the example but the same process applies to FCH₄. The residuals (ϵ) were combined for estimating the log-likelihood in the first-round as so:

$$\epsilon_{T,vpha} = NEE_{T,vpha} - N\hat{E}E_{T,vpha} \tag{2}$$

$$\epsilon_{SA} = NEE_{SA} - N\hat{E}E_{SA} \tag{3}$$

$$\ell = f(\epsilon_{Typha}|\mu_{Typha}, \sigma_{NEE}) + f(\epsilon_{SA}|\mu_{SA}, \sigma_{NEE})$$
(4)

where NEE is measured data, \hat{NEE} is simulated data, ℓ is the log-likelihood, σ_{NEE} is the estimated error parameter, and the subscripts denote the flux source, which at this stage is approximated using the contribution thresholds previously mentioned. We assumed independent Gaussian noise such that the log-likelihood function f is given by:

$$f = -\frac{1}{2} \sum_{i=1}^{n} \frac{\epsilon^2}{\sigma_{NEE}^2} - \frac{1}{2} n \log(2\pi \sigma_{NEE}^2)$$
 (5)

The prior distributions for the second-round were truncated normal prior distributions that were fit to the posterior parameter distributions from the first-round ($P\theta 1$) as they showed approximately normal behaviour. However, the standard deviation of the first-round posterior was doubled when creating the second-round prior distributions to allow for greater flexibility as the first-round used 70% thresholds, where the flux source could be contaminated rather than representing 100% flux sources corresponding to inside and outside the *Typha* plot, respectively

The second-round used all available data and we assumed that the measured (and simulated) NEE or FCH_4 is equal to the flux from the Ty-pha parcel and the SA and scaled by their area weighted contributions CB_{Tvpha} and CB_{SA} :

$$N\hat{E}E = N\hat{E}E_{Typha}CB_{Typha} + N\hat{E}E_{SA}CB_{SA}$$
(6)

The residuals and the log-likelihood for the second-round are then given as:

$$\epsilon = NEE - N\hat{E}E \tag{7}$$

$$\ell = f(\epsilon | \mu, \sigma_{NEE}) \tag{8}$$

and the same log-likelihood function is used as in the first-round. The number of model iterations for the first-round was 2×10^5 and the second-round was 10^5 . An overview of the modelling procedure is provided in Fig. 2.

2.5.1. NEE modelling and flux partitioning

The NEE can be simply decomposed into GPP and R_{eco} , such that:

$$NEE = GPP + R_{eco} (9)$$

using the conventional notation where a negative NEE is uptake of carbon by the land system and a positive NEE is a loss. This can be represented using the hyperbolic light-response curve (LRC) (Falge et al., 2001) and a respiration function for $R_{\rm eco}$:

$$NEE = -\frac{\alpha \beta R_g}{\alpha R_o + \beta} + R_{\text{eco}}$$
 (10)

where α is the light utilisation efficiency of the canopy and is the initial slope of the LRC, R_g is global radiation, and β is the maximum CO_2 uptake rate of the canopy at infinite R_g . R_{eco} is modelled using the respiration-temperature dependence function of Lloyd and Taylor (1994):

$$R_{\text{eco}} = R_{ref} \exp\left(E_0 \left(\frac{1}{T_{ref} - T_0} - \frac{1}{T - T_0}\right)\right)$$
 (11)

where R_{ref} is the reference respiration, E_0 is the temperature sensitivity, T_{ref} is the reference temperature of 15 °C, and T_0 is the zero respiration temperature of -46.02 °C, as fitted by Lloyd and Taylor (1994).

In EC studies, the partitioning of NEE into $R_{\rm eco}$ and GPP is most frequently done with the night-time partitioning method of Reichstein et al. (2005) or daytime partitioning approach of Lasslop et al. (2010). Both of these approaches use sliding windows to fit parameters through time to reflect changes in carbon loss and uptake. Rather than use sliding windows, which would drastically increase the amount of parameters that need to be estimated, a sine term is introduced to represent seasonality in the parameters for GPP:

$$\alpha_{Sin} = \alpha + A_{\alpha} \sin(2\pi(t - \phi)/365) \tag{12}$$

$$\beta_{Sin} = \beta + A_{\beta} \sin(2\pi(t - \phi)/365) \tag{13}$$

$$GPP = -\frac{\alpha_{Sin}\beta_{Sin}R_g}{\alpha_{Sin}R_g + \beta_{Sin}}$$
 (14)

where A_{α} and A_{β} are amplitude scalers for α and β , respectively, t is the day of the year, and ϕ is the phase shift for GPP. These parameters can be expected to vary in time for physiological reasons, where the leaf area index, light absorptivity, and senescence (particularly in annual plants such as Typha) would vary carbon uptake in response to light. A sine term introduction was also tested for $R_{\rm eco}$ parameters but was found to not improve performance as the dependence on temperature was adequate to capture seasonal variability, and therefore the term was not introduced and Eq. (11) was used.

Following Eq. (9), the modelled NEE of the two land uses is therefore given as:

$$N\hat{E}E_{Typha} = GPP_{Typha} + R_{ecoTypha} \tag{15}$$

$$N\hat{E}E_{SA} = GPP_{SA} + R_{ecoSA} \tag{16}$$

where NEE_{Typha} and NEE_{SA} are the simulated NEEs of *Typha* and outside the plot (SA).

For data input into the model, the same PAR was input for R_g in Eq. (14) for both flux sources, however for temperature in the respiration equation (Eq. (11)) surface soil temperature in the top 10 cm as measured in the *Typha* plot and in the reference grassland plot was used for the respective flux sources.

2.5.2. FCH₄

An exponential temperature function with decay for declining water level was used to simulate fluxes of CH₄:

$$FCH_4 = a \exp(bT) \frac{1}{(1 + \exp(-WL))^k}$$
 (17)

where a, b, and k are coefficients on the non-linear equation, T is temperature, and WL is water level. The a (flux at 0 °C) and b (exponent)

parameters define FCH_4 in response to temperature, while k smooths the sigmoidal water level function. The parameter distributions were estimated using the same two round procedure, where uniform priors were used in the first-round with 70% flux source thresholds, followed by using all data in the second-round and combining the two sources using the following equations:

$$F\hat{C}H_{4Typha} = a_{Typha} \exp(b_{Typha}T_{Typha}) \frac{1}{(1 + \exp(-WL_{Typha}))^{k_{Typha}}}$$
 (18)

$$F\hat{C}H_{4SA} = a_{SA} \exp(b_{SA}T_{SA}) \frac{1}{(1 + \exp(-WL_{SA}))^{k_{SA}}}$$
(19)

$$F\hat{C}H_4 = F\hat{C}H_{4Tvpha}CB_{Tvpha} + F\hat{C}H_{4SA}CB_{SA}$$
 (20)

The surface soil temperature and water level as measured in the Typha plot was used for T_{Typha} and WL_{Typha} , respectively, and the surface soil temperature and water level measured in the reference meadow plot, $300\,\mathrm{m}$ southeast of the plot, was used for T_{SA} and WL_{SA} .

2.6. Data and analysis

The posterior parameter sets from the second-round ($P\theta2$) were used to assess the performance of the model framework and for making annual budgets. Annual totals were calculated as the cumulative sum of simulated fluxes for a model year. The uncertainty of the annual totals is shown by the 2.5 and 97.5 quantiles of the annual totals produced by the parameter sets, and we also present the standard deviation of the annual total distribution. The uncertainty due to u* threshold was not assessed, however it is expected to be minimal for simulated fluxes of Typha and SA because the Kljun et al. (2015) model only produces a footprint when u* is more than $0.1\,\mathrm{m\,s^{-1}}$. The uncertainty of the footprint model was not propagated and issues due to footprint model uncertainty are discussed later.

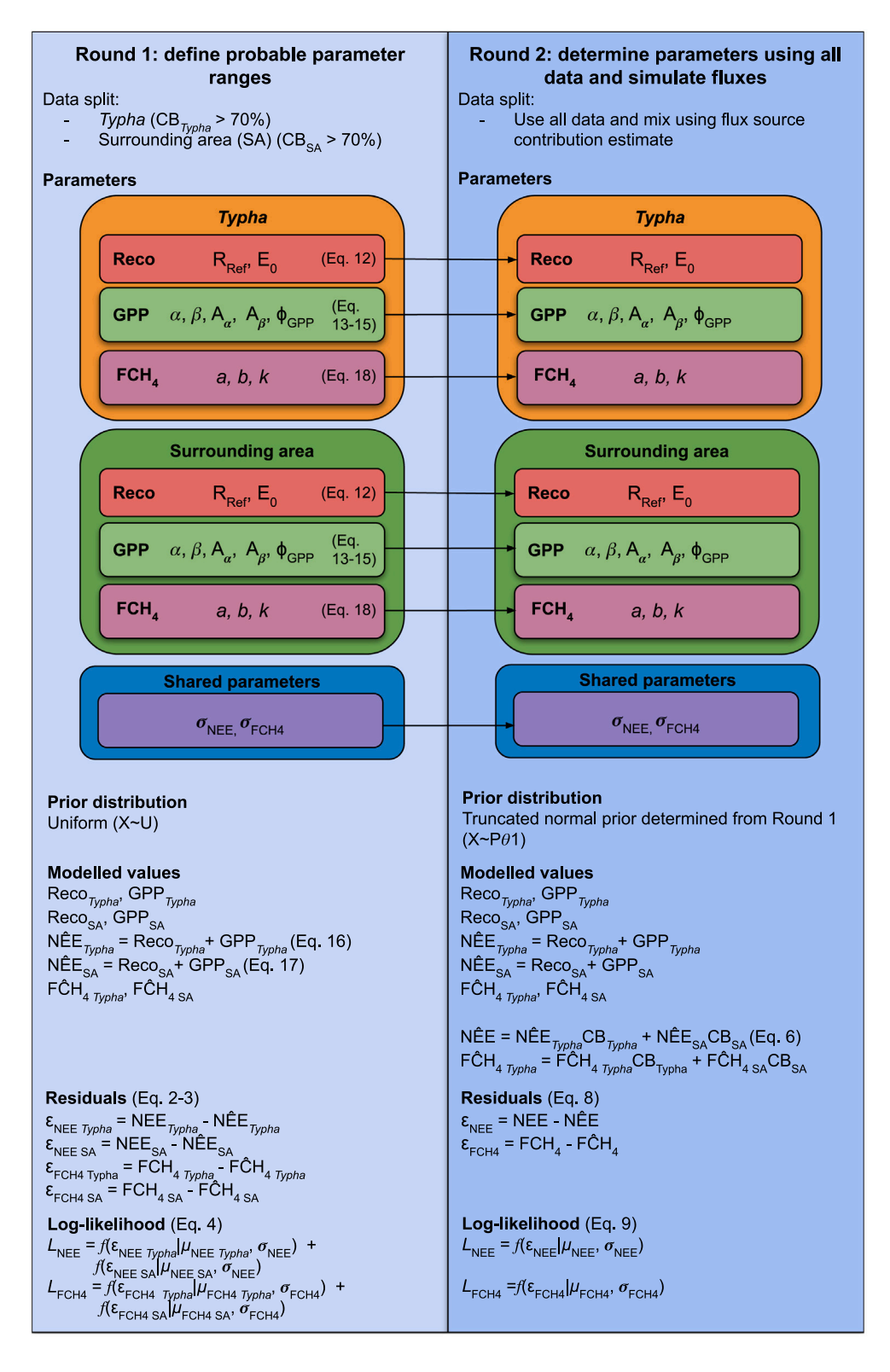
We also compared the output of the Bayesian framework with the standard Marginal Distribution Sampling (MDS) gapfilling (Reichstein et al., 2005) and night-time flux partitioning approach using 70% thresholds for in and outside the *Typha* plot. Since the alternate flux source outside the *Typha* plot is mostly pasture, we also compared the fluxes simulated for outside the plot with fluxes as measured by an EC system that was temporarily located on an adjacent field at Zegveld between May 2021 and August 2021. While the SA is mostly pasture, there are ditches and paths in this area which makes it less representative than the typical area of Zegveld which the temporary EC tower measured, and differences in fluxes were expected due to this. The annual uncertainty of the MDS annual totals was estimated using the mean residual error without considering correlation.

All analysis in this study was done using R (R Core Team, 2022) in combination with R tidyverse packages (Wickham et al., 2019).

3. Results

3.1. Study period

There were seasonal differences in the key meteorological variables and fluxes of CO2 and CH4 over the study period (Fig. 3). Immediately noticeable is the clear annual cycle of northern hemisphere CO2 uptake and emission, where the largest uptake typically occurs during spring and summer, while those seasons also tended to have the highest emissions of CH₄. The year 2022 was a warm year in the Netherlands with a mean annual temperature of 11.6 °C, compared to 2021 which had a mean annual temperature 10.4 °C. Total annual rainfall was lower for 2021 than 2022 at 720 and 814 mm, respectively, however summer totals were 175 and 146 mm, respectively. The water level inside the Typha plot was usually maintained above or near the surface level, except for a period during the August 2022. Mean summer groundwater levels for 2021 were 4 and -72 cm, relative to the ground level, respectively for Typha and SA, while for 2022 they were -1 cm and -88 cm, respectively. The soil temperature in the Typha plot was often lower in summer, likely due to the saturation of the soil.



 $\textbf{Fig. 2.} \ \ \textbf{Overview of the Bayesian inference framework used in this study}.$

3.2. Flux sources

We first inspected the relationship between CB_{Typha} and the fluxes of CO_2 and CH_4 to check if there were clear differences in flux behaviour based on the footprint (Fig. 4). In the relationship between air temperature and night-time NEE, when there was more Typha in the footprint there is a distinct pattern visible and the fluxes generally were lower

and did not increase as rapidly with air temperature. During daytime, there was a larger positive association between CO_2 uptake and PAR as CB_{Typha} increased. There is another distinct curve with high CB_{Typha} that is visible between around PAR 0 to $500\,\mu\mathrm{mol}\,\mathrm{m}^{-2}\,\mathrm{s}^{-1}$ where there is poorer light utilisation efficiency and these values were mostly from autumn and winter when there is Typha senescence. The relationship of air temperature and the FCH₄ was noisier than CO_2 but as temperature

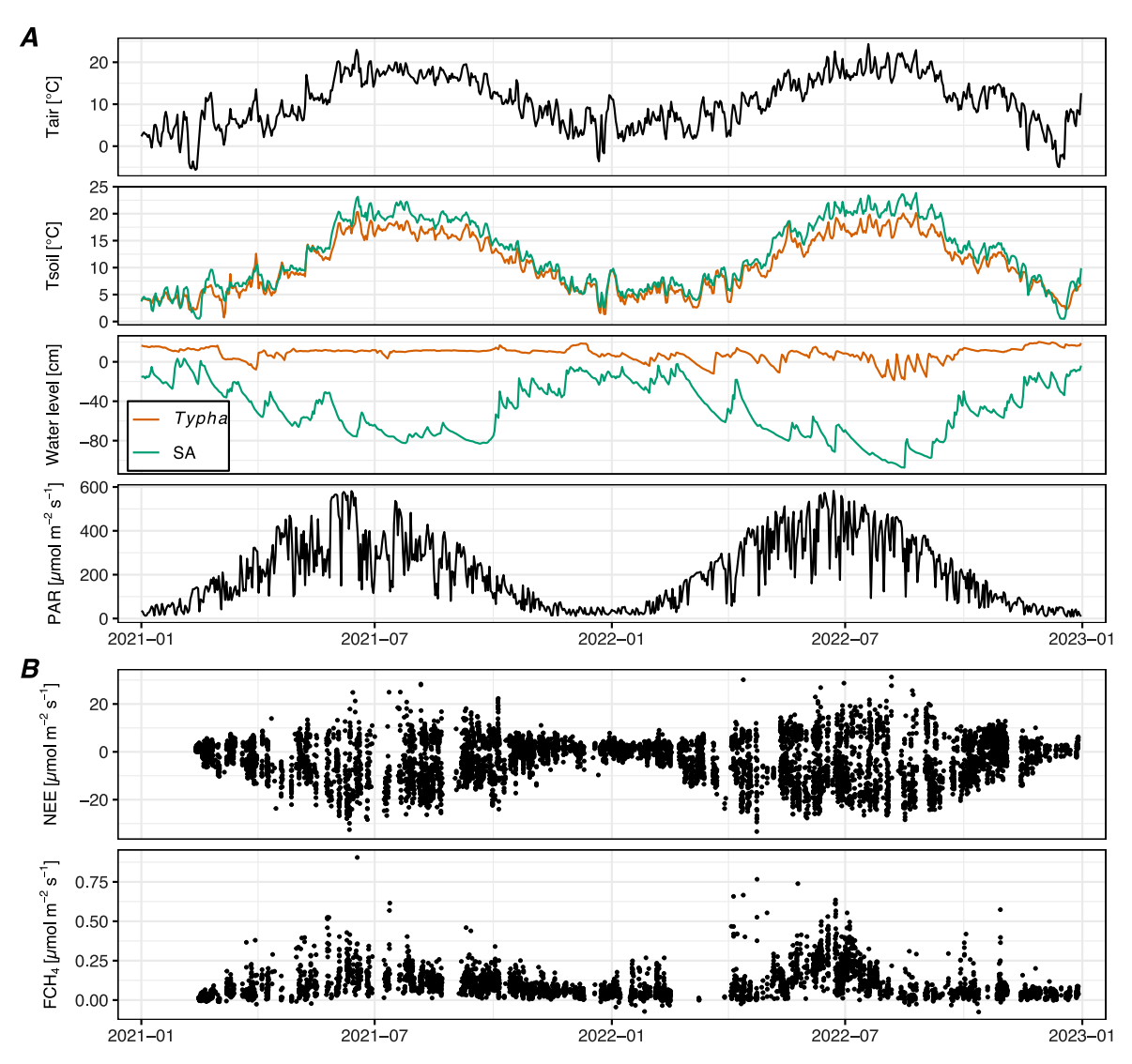


Fig. 3. (A) Daily means of key meteorological variables over the study period. (B) Half-hourly flux observations of the net ecosystem exchange (NEE) (top) and CH₄ (FCH₄) (bottom).

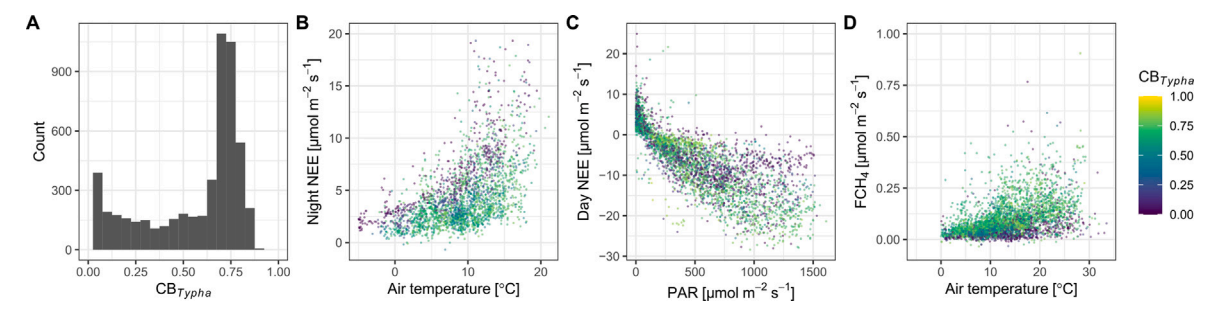


Fig. 4. Plots of (A) histogram of the proportion of the flux estimated to originate from the Typha plot (CB_{Typha}) , (B) night-time net ecosystem exchange (NEE) against air temperature, (C) daytime NEE against photosynthetically active radiation (PAR), and (D) methane flux (FCH₄) against air temperature. The timestep of the points is 30-min.

and CB_{Typha} increases so does the flux. The trafficking of cattle on the property and livestock mowing are also probable sources of spikes of CH_4 emission for low values of CB_{Typha} (and therefore high CB_{SA}).

3.3. Bayesian inference

3.3.1. Parameter distributions and model performance

The posterior distributions of the parameters from the second-round are shown in Fig. 5. The posterior distribution of the first-round, which

were used as the prior distributions for the second round after truncation to the 95% credible interval, are presented in Figure S1. In Figure S1 all parameters showed approximately normal behaviour and clear distributions that could be constrained for fitting in the second-round. A comparison of the first and second-round posterior distributions is presented in Figure S2 which shows that there were no extreme shifts in parameter distributions between rounds but some different optima were found after introducing all data in the second-round.

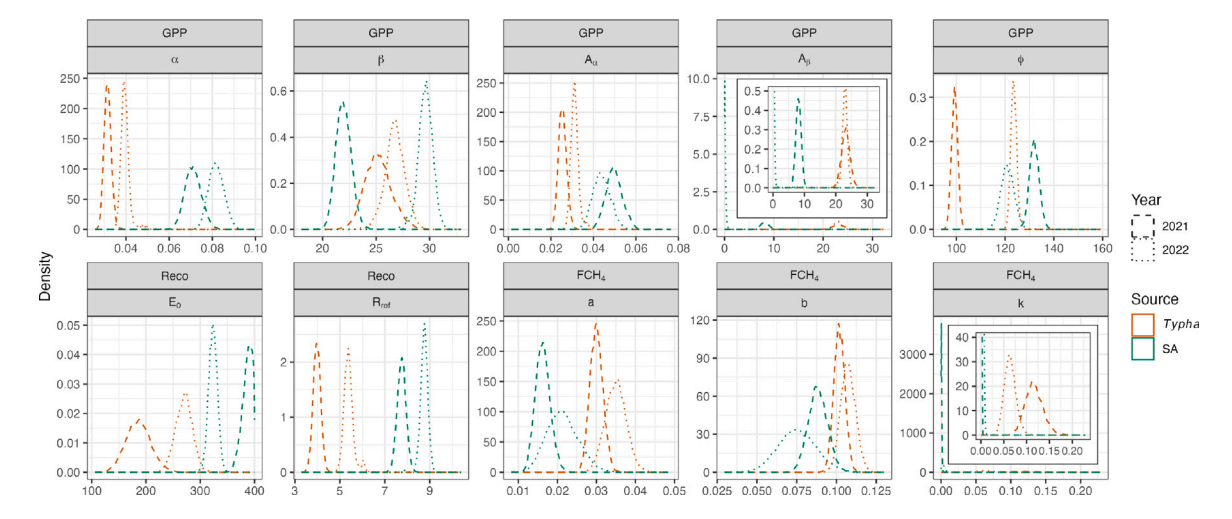


Fig. 5. Posterior distributions of the second-round of CO_2 model parameters of gross primary production (GPP) and ecosystem respiration (R_{eco}), and CH_4 flux (FCH₄) model parameters a, b, and k. An inset is provided for the GPP parameter A_{ij} and FCH₄ parameter k for an enhanced view.

There were clear differences between the two land use classes across nearly all model parameters, but also year-to-year variation (Fig. 5). The GPP light use efficiency parameter α had lower values for Typha compared to SA and also had less annual variability, as shown by the distributions of A_{α} . There was a small difference in the distributions of β for both years for Typha and there was a larger difference for SA, where the distribution was spread across lower values for 2021 than 2022. The distributions of A_{θ} indicated that there is greater annual variability in maximum GPP for Typha compared to SA. The A_{β} parameter had values greater than zero in 2021, however in 2022 the parameter had values around zero, indicating it was not useful for that model year. The distributions of ϕ simply indicate that the annual maximum uptake of GPP shifts from the day of the year 90 when ϕ is 0 to closer towards the middle of the year. For $R_{\rm eco}$, Typha had lower valued distributions for both E_0 and R_{ref} for both years. This would result in lower predicted values of $R_{\rm eco}$ with increasing temperature and is in agreement with the results shown in Fig. 4. The CH₄ soil temperature parameters, a and b, had higher values for Typha than for SA. The parameter k only had distributions more than 0 for *Typha*, indicating that water level was not important for predicting SA CH₄ emissions and that the relationship is controlled by the temperature response parameters a and b.

Model performance statistics were calculated using all the posterior parameter sets of the second-round. Overall, model performance was good for CO_2 (Table 1). The best performing simulation obtained Lin's concordance correlation coefficients (LCCC) of 0.94, R^2 of 0.89, and a root mean square error (RMSE) of 2.98, and general performance across the posterior parameter sets was also satisfactory. Performance was poorer for CH_4 , with the best values of LCCC of 0.57, R^2 of 0.38, and RMSE of 0.05. The mean of the simulations follows the 1:1 line for CO_2 well and does not indicate a strong bias, however for CH_4 the model does not reproduce some higher observed values (Fig. 6), despite having generally low mean bias (Table 1).

3.3.2. Timeseries

There was a clear annual cycle simulated for both land uses (Fig. 7). Typha was a net sink of CO_2 during the warmer seasons and was only a net source in the winter, early spring and autumn. In contrast, SA was simulated to be a net sink from the onset of spring until late spring to early summer, and was then simulated to be a net source. Simulated daily emissions of CH_4 were higher for Typha than SA, with the highest emissions coming in the warmer seasons. There is a clear difference in the rate of annual emissions in 2022 compared to 2021, which corresponds to a hotter year compared to a mild one, respectively. Of interest, there is a noticeable decrease in observed CH_4 emissions 2022

Table 1 Summary of the model performance of the CO_2 flux (NEE) and CH_4 flux (FCH₄). The model quality criteria are the root mean square error (RMSE), coefficient of determination (R^2), Lin's concordance correlation coefficient (LCCC), and mean bias.

Flux	Stat	RMSE	\mathbb{R}^2	LCCC	Bias
NEE	Min	2.98	0.78	0.88	-0.749
	Q2.5	2.99	0.85	0.92	-0.265
	Median	3.01	0.85	0.92	-0.091
	Q97.5	3.03	0.89	0.94	0.094
	Max	4.34	0.89	0.94	0.256
FCH_4	Min	0.05	0.24	0.27	-0.043
	Q2.5	0.05	0.28	0.40	0.001
	Median	0.08	0.29	0.44	0.003
	Q97.5	0.10	0.38	0.56	0.009
	Max	0.11	0.38	0.57	0.035

after day 200, which corresponds to a period where the water level in the Typha plot was not maintained above the surface and decreased past 20 cm below the surface, as is visible in Fig. 3. Timeseries of $R_{\rm eco}$ and GPP are provided in Figure S3.

The timeseries of the temporary EC tower on the nearby meadow at Zegveld and the simulation of SA is provided in Figure S4. The simulation tracks the observed points, obtaining a LCCC of 0.80 and an R^2 of 0.67, but tends to underestimate uptake of CO_2 . Possible reasons for the underestimation are that the simulation only uses inflexible annual scale equations, despite the introduction of the sine wave in the GPP parameters, and that there is a greater proportion of ditch area in the SA footprint compared to the temporary EC site, where GPP would likely be lower and $R_{\rm eco}$ higher. The timeseries of CH_4 also appears to simulate the average emission but does not capture the emission dynamics and only obtained LCCC and R^2 scores of 0.04 and 0.02, respectively.

The comparison of the Bayesian inference approach and the threshold filtered and gapfilled timeseries using the MDS method are presented in Figure S5 for $\rm CO_2$ and Figure S6 for $\rm CH_4$. The Bayesian approach showed greater $\rm CO_2$ uptake in the growing season by Typha and slightly higher emissions in the cooler months. The timeseries of the two approaches for SA are broadly similar, with the MDS gapfilled series showing generally greater extremes. The Typha $\rm CH_4$ were frequently higher in the Bayesian approach than the MDS gapfilled timeseries, and it also did not simulate a drop in emissions after July 2022 as the MDS approach showed. The Bayesian SA $\rm CH_4$ timeseries had higher emissions in the cooler months. In 2021 they both had similar emissions in the warmer season, but in 2022 the emissions were lower.

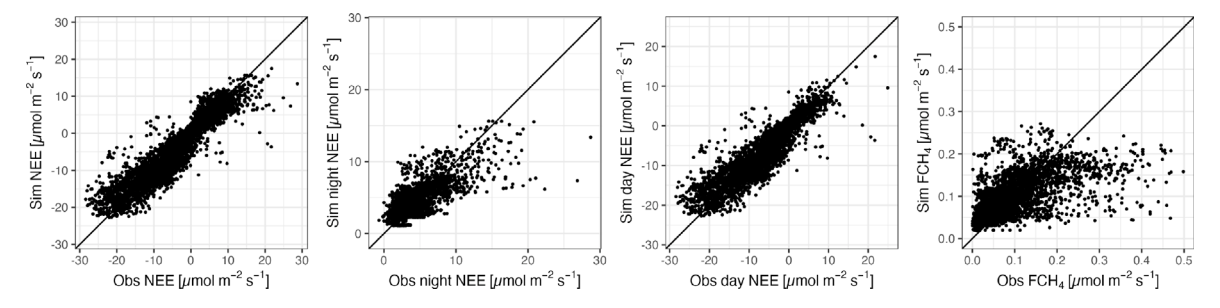


Fig. 6. From left to right: observed and simulated plots of net ecosystem exchange (NEE) of CO_2 for all data, night only, day only, and CH_4 flux (FCH₄) for all data. The black line is the 1:1 observed and simulated relationship. The means of the simulated values are presented in this plot.

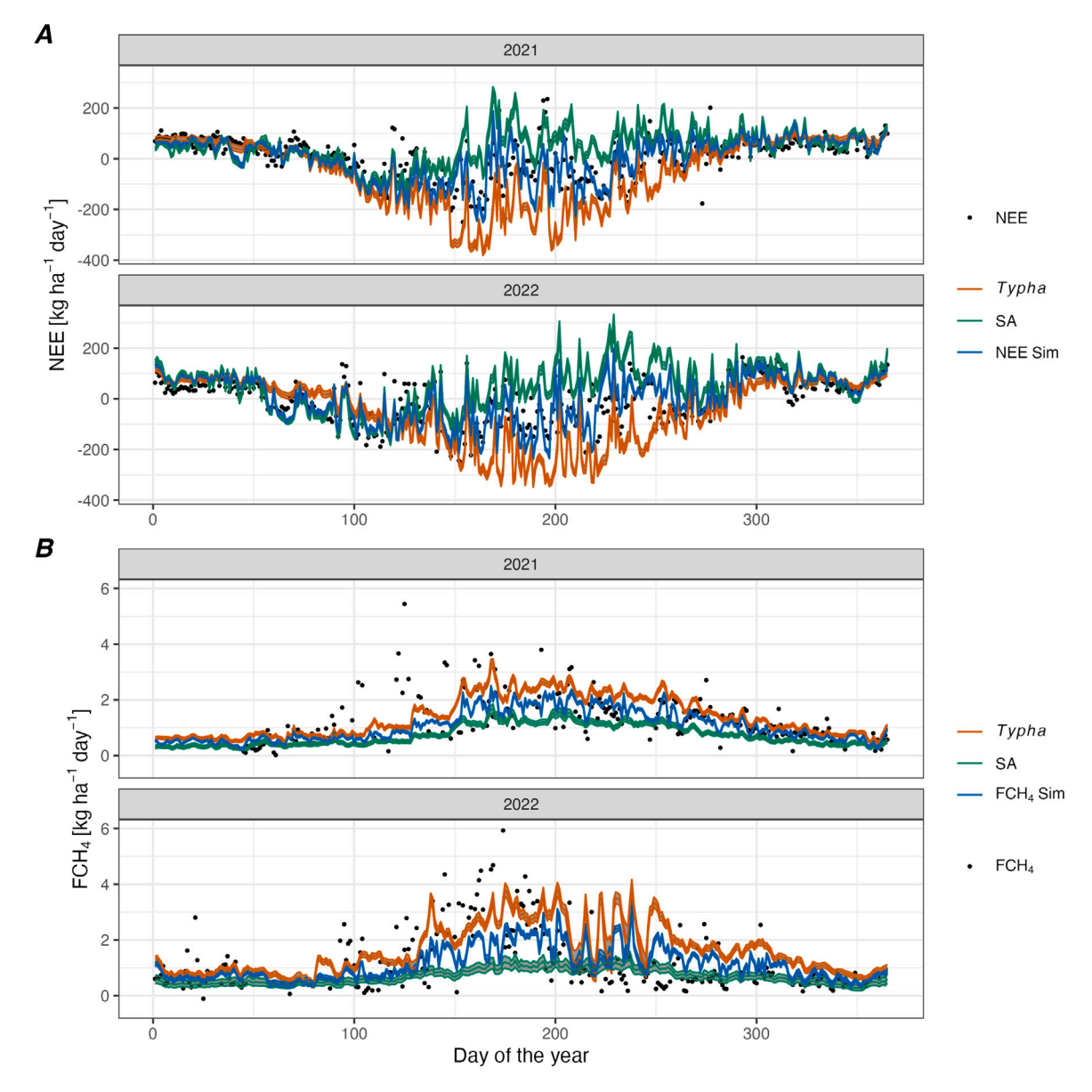


Fig. 7. Modelled fluxes of the net ecosystem exchange (NEE) of (A) CO_2 and (B) CH_4 for Typha (red), surrounding area (SA) (green), and the NEE as would be observed by the tower (blue). The width of lines represents the 2.5% to 97.5% simulation ranges. The black points are daily aggregates of the observed fluxes, which were gapfilled with the MDS algorithm to avoid large biases.

3.3.3. Annual budgets

Budgets were calculated for each year using the simulated timeseries from all posterior parameter sets of the second-round (Table 2). Imports and exports, such as carbon import via irrigation water and harvest, are not considered in these totals. The *Typha* site was simulated to have a net uptake of CO_2 in both 2021 and 2022 with mean NEE values of -18.5 and $-17.8\,\mathrm{t}\,CO_2\,\mathrm{ha}^{-1}\,\mathrm{yr}^{-1}$, respectively, while SA was a net emitter at 16.8 and $17.4\,\mathrm{t}\,CO_2\,\mathrm{ha}^{-1}\,\mathrm{yr}^{-1}$, respectively. R_{eco} was simulated to be almost twice as much for SA compared to Typha, where the average of both simulation years for Typha was 50.5 for Typha and

Table 2 Annual budgets of CO_2 and CH_4 for Typha and surrounding area (SA), presented as the mean and one standard deviation. Budgets of CH_4 and the greenhouse gas (GHG) balance are expressed in CO_2 -equivalents using the 100-year non-fossil global warming potential of 27.0 (IPCC, 2021).

Year	Stat	Reco		GPP		NEE		FCH_4		GHG Balance	:
		t CO ₂ ha ⁻¹ year ⁻¹ t CO ₂ -eq ha ⁻¹ year ⁻¹									
		Typha	SA	Typha	SA	Турћа	SA	Турһа	SA	Турћа	SA
2021 2021	Q2.5 Mean ± SD	40.5 44.2 ± 1.9	86.4 90.8 ± 2.3	-64.9 -62.7 ± 1.1	-76.8 -74.1 ± 1.4	-21.3 -18.5 ± 1.5	13.8 16.8 ± 1.5	13.1 13.6 ± 0.3	6.5 7.1 ± 0.3	-8.2 -4.9 ± 1.5	20.3 23.9 ± 1.5
2021	Q97.5	47.9	95.2	-60.6	-71.2	-15.7	19.7	14.1	7.7	-1.6	27.4
2022 2022 2022	Q2.5 Mean ± SD Q97.5	52.9 56.8 ± 2.4 63.3	105.3 109.3 ± 2 113.1	-78.4 -74.6 ± 1.5 -72.3	-94.2 -92 ± 1.1 -89.7	-20.6 -17.8 ± 1.5 -14.6	14.3 17.4 ± 1.5 20	15 15.9 ± 0.5 16.8	5.7 6.8 ± 0.6 7.9	-5.6 -2 ± 1.6 2.2	20 24.2 ± 1.6 27.9

Table 3

Annual flux totals of CO₂ and CH₄ filtered for minimum contributions of at least 70% from Typha and surrounding area (SA) and gapfilled using the marginal distribution sampling (MDS) algorithm. The annual totals derived by the Bayesian inference approach are provided for comparison.

Year	Method	NEE			FCH_4	FCH ₄			GHG balance	GHG balance	
		t CO ₂ ha ⁻¹ yr ⁻¹				t CO ₂ -eq ha ⁻¹ yr ⁻¹					
		n	Турћа	n	SA	n	Typha	n	SA	Typha	SA
2021 2021	Bayesian MDS	4062 1235	-18.5 ± 1.5 -9 ± 3.5	4062 830	16.8 ± 1.5 17 ± 6.2	3140 999	13.6 ± 0.3 11 ± 0.6	3140 585	7.1 ± 0.3 5.8 ± 1.3	-4.9 ± 1.5 2 ± 3.6	23.9 ± 1.5 22.8 ± 6.3
2022 2022	Bayesian MDS	4584 1130	-17.8 ± 1.5 -6.8 ± 3.7	4584 1170	17.4 ± 1.5 15.9 ± 3.8	2779 800	15.9 ± 0.5 12.5 ± 0.8	2779 419	6.8 ± 0.6 6.3 ± 3.3	-2 ± 1.6 5.7 ± 3.8	24.2 ± 1.6 22.2 ± 5

 $100.5\,\mathrm{t\,CO_2\,ha^{-1}\,yr^{-1}}$ for SA. Annual totals of GPP were also simulated to be higher for SA than *Typha* for both years. The emission by $R_{\rm eco}$ and GPP uptake were lower in wetter and cooler 2021, compared to the hotter and drier year in 2022.

Annual totals of FCH $_4$ have been converted to CO $_2$ equivalents using the non-fossil global warming potential of 27.0 (IPCC, 2021). Emissions of FCH $_4$ were lower in 2021 than 2022 for Typha, with values of 13.6 and 15.9 t CO $_2$ -eq ha $^{-1}$ yr $^{-1}$, respectively, whereas the emissions were similar for both years for SA at 7.1 and 6.8 t CO $_2$ -eq ha $^{-1}$ yr $^{-1}$. The GHG balance provided is the addition of the annual NEE and FCH $_4$ totals. The Typha site had a net negative GHG balance of in 2021 and 2022 at -4.9 and -2.0 t CO $_2$ -eq ha $^{-1}$ yr $^{-1}$, respectively. SA was a net positive GHG balance for both years with annual totals of 23.9 and 24.2 t CO $_2$ -eq ha $^{-1}$ yr $^{-1}$.

Annual totals derived from the Bayesian and MDS methods were similar for both NEE and FCH₄ for SA (Table 3). For Typha, the difference between methods of NEE was 9.5 and $11.0\,\mathrm{t}\,\mathrm{CO}_2\,\mathrm{ha}^{-1}\,\mathrm{yr}^{-1}$ for 2021 and 2022, respectively, while FCH₄ differed by 2.6 and $3.4\,\mathrm{t}\,\mathrm{CO}_2\text{-eq}\,\mathrm{ha}^{-1}\,\mathrm{yr}^{-1}$ for 2021 and 2022, respectively. In Table 3, the number of data points available for parameter estimation or gapfilling for the different methods are also presented and it highlights the greater number of data points that the Bayesian inference approach has as information for the modelling process.

4. Discussion

4.1. Interpretation of fluxes and annual budgets

The results showed that Typha paludiculture was a net CO_2 sink and SA, primarily a dairy meadow on peat soil, a source of CO_2 , while the CH_4 emissions of Typha paludiculture were approximately double compared to the SA. The GHG balances shown in Table 2 indicate that Typha paludiculture would have a net cooling effect on the climate compared to the meadow when using the 100-year GWP of CH_4 , and the net emissions were 28.8 and $26.2\,t\,CO_2$ -eq ha⁻¹ yr⁻¹ lower across the two simulation years. Even though the uncertainty was relatively large, as indicated by the difference from the Q2.5 to Q97.5 quantiles of around 5 to $7\,t\,CO_2$ -eq ha⁻¹ yr⁻¹ for the annual totals of NEE for both land uses, the relative difference between the two land uses was greater. These balances do not include biomass harvest (carbon export), carbon import via irrigation water, or potential nitrous oxide emissions, and if these extra factors were considered there is the possibility that the

interpretation could change. However, in our case the export of biomass of the *Typha* is intended for longer term stores, namely as building insulation material (Wichtmann et al., 2016; Lahtinen et al., 2022), and the end result is unlikely to be different.

Studies on Typha paludiculture are limited and there are few reports of annual flux totals. Another study in the Netherlands reported one year of annual totals for a pilot paludiculture project where chamber measurements were conducted on T. latifolia (van den Berg et al., 2024). In their study, the prior land use was also a drained meadow and topsoil was excavated before rewetting, van den Berg et al. (2024) reported annual totals of $R_{\rm eco}$, GPP, and NEE of $47.2\,{\rm t\,CO_2\,ha^{-1}\,yr^{-1}}$, $-64.5 \text{ t CO}_2 \text{ ha}^{-1} \text{ yr}^{-1}$, and $-17.2 \pm 15.0 \text{ t CO}_2 \text{ ha}^{-1} \text{ yr}^{-1}$ (mean $\pm \text{SD}$ were only provided for NEE). These totals compare remarkably well with the range of annual emissions reported in our study, however there is a large variation amongst the replicates for NEE. van den Berg et al. (2024) also reported annual totals of T. angustifolia where the annual totals of R_{eco} , GPP, and NEE were 27.8 t CO₂ ha⁻¹ yr⁻¹, -51.5 t CO₂ ha⁻¹ yr⁻¹, and $-23.7 \pm 19.0 \,\mathrm{t}\,\mathrm{CO}_2\,\mathrm{ha}^{-1}\,\mathrm{yr}^{-1}$, respectively, and highlights that there can be large interspecies differences in emission rates. Other studies have reported annual totals of Typha in natural or in rewetted natural systems. The annual totals of GPP for Typha are comparable to values found in a California marsh dominated by T. latifolia of between 42 to $73 \, \mathrm{t} \, \mathrm{CO_2} \, \mathrm{ha^{-1}} \, \mathrm{yr^{-1}}$ (Rocha and Goulden, 2009), and values of R_{eco} are also comparable, as inferred from the results of net primary production (NPP) of 26 to 46 t CO₂ ha⁻¹ yr⁻¹. Lower values are also found in literature, where Minke et al. (2016) reported a range for NEE of -4.1 to 5.5 t CO₂ ha⁻¹ yr⁻¹ from a rewetted fen vegetated with *Typha latifolia* and Hydrocharis morsus-ranae (European frog-bit) in Belarus. The low annual totals of $R_{\rm eco}$ found for the *Typha* parcel in this study, and in others (e.g., Minke et al., 2016; van den Berg et al., 2024), can be explained by the near-permanent inundation of the soil which limits heterotrophic respiration.

The annual values of NEE for the SA were high, but similar to the annual totals for $R_{\rm eco}$ and GPP reported for Dutch peatland grazed meadows by Weideveld et al. (2021), where annual values of chamber fluxes were 100.8 ± 11 and $128.4\pm4.6\,{\rm t\,CO_2\,ha^{-1}\,yr^{-1}}$ for $R_{\rm eco}$ and -89.2 ± 13 and $-65.7\pm4.9\,{\rm t\,CO_2\,ha^{-1}\,yr^{-1}}$ for GPP. The results are also broadly similar to values reported for German peat soils of a NEE of $19.9\pm16.1\,{\rm t\,CO_2\,ha^{-1}\,yr^{-1}}$ by Tiemeyer et al. (2016). In the study of Tiemeyer et al. (2016), they reported mean values of $R_{\rm eco}$ and GPP of $81.4\pm30.4.6$ and $-61.2\pm19.1\,{\rm t\,CO_2\,ha^{-1}\,yr^{-1}}$, where the mean values are lower than reported in this study but within the uncertainty

limits. Another study with automatic chambers on Dutch peat meadows reported net annual uptake of NEE with values ranging between -5.4 to -21.7 t CO_2 ha⁻¹ yr⁻¹ (Boonman et al., 2021), highlighting the spread and potential spatial variability of results. The presence of the drainage ditch in the SA footprint was also a likely cause of high annual $R_{\rm eco}$ and NEE totals in our study as they are a strong source of emissions (Schrier-Uijl et al., 2011; Hendriks et al., 2024).

For CH₄, van den Berg et al. (2024) reported higher annual emissions of T. latifolia of 22.9 \pm 13 t CO₂-eq ha⁻¹ yr⁻¹, but there was a high variation between sample replicates as shown by the standard deviation. Mean annual emissions of T. angustifolia were lower at $10.0 \pm 5.4 \,\mathrm{t}\,\mathrm{CO}_2$ -eq ha⁻¹ yr⁻¹, but similarly had a large variation. The large variation in totals amongst chamber replicates for CH₄, but also with CO₂, also demonstrates of the benefit of measuring at the ecosystem scale with EC. Annual totals of sites dominated by T. latifolia of 7.8 to $10.5 \, t \, \text{CO}_2$ -eq ha⁻¹ yr⁻¹ have been reported for a rewetted Irish cut over bog (Wilson et al., 2007, 2009), 1.1 to 3.5 t CO₂-eq ha⁻¹ yr⁻¹ in a rewetted German fen (Günther et al., 2015), and Franz et al. (2016) reported $10.8 \,\mathrm{t}\,\mathrm{CO}_2$ -eq ha $^{-1}\,\mathrm{yr}^{-1}$ for a shallow German lake. Emissions from SA were high for a meadow, however as mentioned there is a drainage ditch that runs alongside the parcel and was likely a source of CH₄. Annual CH₄ emissions of drained agricultural land with ditches in the Netherlands have been observed to range between 4.0 to $5.5 \, t \, \text{CO}_2$ -eq ha⁻¹ yr⁻¹ and approximately 60 to 70% of emissions originated from ditches and bordering edges of fields (Schrier-Uijl et al., 2011). Ditches are known hotspots of CH₄ emissions globally (Peacock et al., 2021). The trafficking of cattle on the farm was also a possible contributing source of emissions for the SA.

4.2. Modelling approach

Our modelling approach was based on using the flux footprint to weight the source areas and relate it to the measured flux. Previous studies have found that it is difficult to partition fluxes using footprint models (e.g., Wohlfahrt et al., 2012; Chu et al., 2021). In our study, we had strongly contrasting source areas and this translated into detectable differences in flux behaviour with varying footprint coverage (Fig. 4), and subsequently into the parameter distributions and resulting timeseries and annual flux totals. The annual budget results were comparable to values in literature, demonstrating that the modelling process grasped real signals and is useful in mixed footprint settings such as the one studied, and thereby we succeeded to meet our first aim.

Other studies have decided to truncate the footprint to 80% of the source weight contour with only a marginal influence on the final results (Kim et al., 2018; Chu et al., 2021). In our study, the surrounding SA the results of the Bayesian inference approach and the traditional approach yielded similar net annual GHG balance totals, where the differences between the methods was 1.1 and $2.0 \,\mathrm{t}\,\mathrm{CO}_2$ -eq ha⁻¹ yr⁻¹ in 2021 and 2022, respectively. However, for the relatively small experimental Typha plot the differences between the approaches were larger, where the differences between the approaches were -6.9 and -7.7 t CO_2 -eq ha⁻¹ yr⁻¹ in 2021 and 2022, respectively (Table 3). There are two main important reasons for the difference. Firstly, the advantage of our modelling approach is that it could use more data points to grasp likely parameter values and therefore have higher certainty in the flux behaviour of the two land uses in our study (Table 3). Secondly, in the distribution of CB_{Typha} there were few data points with high values. The total number of data points exceeding 70% was n = 2423, above 80% n = 400, and above 90% there were zero points. On the other hand, the total number of points below 30% was n = 2018, below 20% was n = 1724, and below 10% n = 1384 points. The lack of values with high footprint contributions for Typha indicates that the threshold filtered and MDS gapfilled approach would have a bias in the fluxes due to the lack of consideration of weighted flux source scaling in the flux estimation. This shows that accounting for footprint heterogeneity

when EC towers are used for relatively small experimental sites, where there may be markedly different behaviour between land uses, is crucial for GHG budget estimation.

We used a conventional function for $R_{\rm eco}$ but modified the GPP function with an annual sine wave to allow the parameters to vary smoothly through the year. The sine parameters, A_{α} and A_{β} , were found to be useful except in one case where values A_{θ} for SA in 2022 were close to zero, indicating for one year there was little annual variability in maximum GPP uptake by SA. This may be explained by poor seasonal coverage of data when determining the first-round prior distributions. The use of the sine terms proved important for Typha, particularly for β_{sin} , as demonstrated by the posterior distribution of A_{β} for Typha had higher values than SA (Fig. 5), which means larger changes in maximum GPP throughout the year. This is unsurprising, given that Typha is an annual crop while grass is perennial. Instead of using a sine curve, an alternate indicator of vegetation status or productivity could be used, such as the normalised difference vegetation index (NDVI) or leaf area index (LAI), as a scaling parameter. In our case, we did not have continuous estimates of NDVI or LAI locally and gaps in remotely sensed data were too large. In addition, other functions than the sine function tested here may provide suitable or better fits of the data, e.g., a Gaussian function since it can more flexibly accommodate the growing season length compared to a more rigid sine function.

There is no standardised approach for gapfilling or simulating CH_4 fluxes but using simple empirical relationships is common and can often provide a reasonable fit (e.g., Rinne et al., 2007; Schrier-Uijl et al., 2010; Levy et al., 2012; Schrier-Uijl et al., 2014; Turetsky et al., 2014). Machine learning methods can be considered the state of the art as they can better handle multiple predictors and the nonlinearity and hysteresis of CH_4 emissions (Knox et al., 2015, 2019; Kim et al., 2020; Irvin et al., 2021; Staudhammer et al., 2022). We used a simple temperature and water level dependence relationship here for parsimony, but alternate functions that also incorporate extra predictors should be tested and may see performance gains. How a more complex machine learning approach could be integrated into the framework presented should be explored for more enhanced simulation of FCH_4 (Wall et al., 2020; Goodrich et al., 2021).

Empirical equations were evaluated in the Bayesian framework at the annual scale to reduce the parameter burden and for the simpler evaluation of our approach. Parameter estimation could be attempted seasonally, monthly, or even fortnightly, but there would need to be a necessary amount of data collected from multiple source areas over those periods. Parameters could also be interpolated between periods when there is missing data from the source area, as is done by Reichstein et al. (2005). This may be easier if a frequentist inference approach was adopted rather than a Bayesian one.

4.3. Uncertainties and future work

The assumptions of the Kljun et al. (2015) footprint model were not strictly adhered to in this study. The model uses Monin-Obukhov similarity theory and assumes a logarithmic wind profile which are only valid in areas with horizontal homogeneity. In our study, the abrupt change in canopy height between the Typha and SA would cause disturbance to the flow field and violates those assumptions. The disturbance to the flow field will also affect the measurement of fluxes (Huang et al., 2011). EC studies with large canopy discontinuities have focussed on forest edges (e.g., Klaassen and Sogachev, 2006; Sogachev et al., 2008; Belcher et al., 2012; Kanani-Sühring and Raasch, 2015) where there is a much larger canopy height difference (typically at least 10 times) and different structural properties, such as vegetation density, than in our study. We inspected disturbances to the flow field by comparing the half-hourly wind speeds from different wind directions as measured at the EC tower location and at the meteorological station at Zegveld which surrounded by a near-homogeneous meadow across seasons. The residuals between the measurements show greater disturbance (lower wind speed) between the two locations when the wind flows over the Typha parcel (Figure S7), which is expected due to the higher canopy height, however there is still a bias when the wind flows over the meadow towards the EC tower. Differences range from -0.28 to $-0.49\,\mathrm{m\,s^{-1}}$ when the wind comes from the south east over the meadow and decrease to -0.81 to $-1.18\,\mathrm{m\,s^{-1}}$ when the wind direction is over the *Typha*. When the wind is approximately between abrupt change between 160 to 180 degrees, the median difference is $-0.83 \,\mathrm{m\,s^{-1}}$ and there also appears to be more outliers. In addition, the residuals are the smallest in spring across all wind sectors, which is after the *Typha* harvest and the canopy height differential is also the smallest. While a small difference may be expected between the measurement locations and/or due to different instruments, the values here show that a bias exists in the measurements that would affect the calculation of the turbulent flux and also affect footprint estimation and this bias remains unquantified.

The calculation of the flux and shape of the flux footprint is influenced by the displacement height and roughness length (Arriga et al., 2017). The values of the displacement height and roughness length were derived from the canopy height of the Typha for each timestep, even when the wind was not coming directly over the Typha canopy, despite there being a maximum difference of around 1.8 m for a part of the year to the surrounding meadow area. This was done because Typha was a smaller experimental parcel and it was easier to define CB_{Typha} , and therefore CB_{SA} . It would not be trivial to vary the displacement height or roughness length parameters depending upon the wind direction and particularly when the flux is likely to originate from multiple source areas. This has likely introduced some bias and uncertainty in our approach that remains unquantified. Moreover, the uncertainty of footprint models becomes larger as the upwind distance from the measuring point increases (Kljun et al., 2015). This may lead to issues with incorrect flux source attribution, which is important for the parameter identification and mixing process in our method. More complex footprint models than the flux footprint prediction model of Kljun et al. (2015) as used here may be able to deal with aforementioned issues, but at the expense of simulation complexity and much greater computation time (Leclerc and Foken, 2014). Nevertheless, we showed that multiple source areas could be parameterised well, but more work needs to be done to inspect and deal with these potential issues.

The height of our sonic anemometer was also closer to the canopy height than conventionally desired. The best practical position for an EC tower is in the constant flux layer starting around 1.2–2 canopy heights above the ground and at least 1–2 m above the canopy (Aubinet et al., 2012). In our measurement site, we may have been measuring in the roughness sublayer when the *Typha* grew to its maximum height for potentially 3 to 4 months per year. The height of the tower was chosen to maximise the source area of the *Typha* field with the prevailing wind direction of south-west, given that it is a relatively small parcel at 0.4 ha. While the *Typha* parcel is relatively small, it is still one of the largest, if not the largest, paludiculture trial fields in the Netherlands. The approach in our study may be experimental, but this study site presented itself as an ideal location to test this framework and to try and improve the annual estimate of fluxes for the *Typha* plot and improve the understanding of GHG exchange of paludiculture.

Evaluating our modelling approach at more sites would test the rigour of the framework and may reveal more insights into GHG exchange in heterogeneous sites. Testing with more than two source areas would also be interesting if there is sufficient data to do so. Further experimental validation by, for example, using longer timeseries of multiple EC towers would be valuable.

5. Conclusions

We presented a novel Bayesian inference approach of extracting useful flux information from all timesteps to constrain flux behaviour and annual budgets in situations with heterogeneous field sites. We anticipate that this approach is useful in situations where there are, for example, contrasting vegetation types, water levels, or particular field treatments that would lead to detectable differences in flux behaviour by a single eddy covariance tower. Addressing our original aims: (1) In our test case, a paludiculture trial next to a dairy meadow and ditches, the Bayesian inference approach could take advantage of many more data points and identified probable parameter distributions well. (2) Our results showed good performance at simulating CO2 fluxes, but performance for CH₄ fluxes was relatively poorer. Compared to a traditional threshold filtering and standard gapfilling approach, our Bayesian inference method produced comparable timeseries and annual budgets for the dairy meadow and ditches, but differences found for Typha were most likely due to the greater number of data points and source strength scaling included in the Bayesian approach. (3) We found that the Typha paludiculture land use had a net uptake of CO2 and higher emissions of CH4 than the meadow. Overall paludiculture had a more favourable net annual greenhouse gas balance, excluding carbon imports and exports, of 28.4 and 26.2 t CO₂-eq ha⁻¹ yr⁻¹ in our two study years of 2021 and 2022 compared to the surrounding dairy meadow and ditches. This suggests that, in our case, paludiculture with Typha latifolia is a viable strategy to reduce peat oxidation and net GHG emissions. Future work should evaluate more source areas, across a wider range of conditions, and try to use a longer timeseries with multiple towers to further validate simulated fluxes.

CRediT authorship contribution statement

Alexander J.V. Buzacott: Writing – review & editing, Writing – original draft, Software, Methodology, Investigation, Formal analysis, Data curation. Merit van den Berg: Writing – review & editing. Bart Kruijt: Writing – review & editing. Jeroen Pijlman: Writing – review & editing. Christian Fritz: Writing – review & editing. Pascal Wintjen: Writing – review & editing. Ype van der Velde: Writing – review & editing, Project administration, Conceptualization.

Declaration of competing interest

The authors declare the following financial interests/personal relationships which may be considered as potential competing interests: Alexander Buzacott reports financial support was provided by the Dutch Ministry of Agriculture, Nature, and Food (LNV). If there are other authors, they declare that they have no known competing financial interests or personal relationships that could have appeared to influence the work reported in this paper.

Data availability

Data and Bayesian analysis code are available at this Git repository https://github.com/buzacott/ZegveldBayesianFluxes.

Acknowledgements

This study was conducted as part of the Netherlands Research Programme on Greenhouse Gas Dynamics in Peatlands and Organic Soils (in Dutch: Nationaal onderzoeksprogramma broeikasgassen veenweiden (NOBV)) that was funded by the Dutch Ministry of Agriculture, Nature, and Food (LNV). We sincerely thank the reviewers for their helpful comments which improved our manuscript.

Appendix A

The model parameters and their ranges used for simulating CO_2 and CH_4 in the Bayesian inference approach are presented in Table A.1. The ranges of the parameters were chosen based on common ranges in literature for CO_2 fluxes (e.g., Lasslop et al., 2010; Wutzler et al., 2018), and for FCH_4 they were selected to be wide enough through iteration.

Table A.1Parameters and their ranges used for the Bayesian inference procedure.

Flux	Variable	Parameter	Units	Lower	Upper
NEE	R _{eco}	R _{ref}	μmol CO ₂ m ⁻² s ⁻¹	0	max(NEE _{night})
		E_0	-	50	400
	GPP	α	μ mol CO ₂ J ⁻¹	0	0.22
		β	μ mol CO $_2$ m $^{-2}$ s $^{-1}$	0.001	250
		A_{α}	-	0	0.11
		A_{β}	-	0	50
		$\phi^{'}$	-	0	180
	Error	σ_{NEE}	$\mu mol~CO_2~m^{-2}~s^{-1}$	$0.02\sigma_{NEE}$	$2\sigma_{NEE}$
FCH_4	_	a	$\mu mol~CH_4~m^{-2}~s^{-1}$	0	0.5
	_	b	$^{\circ}C^{-1}$	0	0.5
	_	k	_	0	1
	Error	σ_{FCH_4}	$\mu mol~CH_4~m^{-2}~s^{-1}$	$0.02\sigma_{F\mathrm{CH_4}}$	$2\sigma_{FCH_4}$

Appendix B. Supplementary data

Supplementary material related to this article can be found online at https://doi.org/10.1016/j.agrformet.2024.110179.

References

- Arriga, N., Rannik, Ü., Aubinet, M., Carrara, A., Vesala, T., Papale, D., 2017. Experimental validation of footprint models for eddy covariance CO2 flux measurements above grassland by means of natural and artificial tracers. Agricult. Forest. Meterol. 242, 75–84. http://dx.doi.org/10.1016/j.agrformet.2017.04.006.
- Aubinet, M., Grelle, A., Ibrom, A., Rannik, Ü., Moncrieff, J., Foken, T., Kowalski, A.S., Martin, P.H., Berbigier, P., Bernhofer, C., Clement, R., Elbers, J., Granier, A., Grünwald, T., Morgenstern, K., Pilegaard, K., Rebmann, C., Snijders, W., Valentini, R., Vesala, T., 1999. Estimates of the annual net carbon and water exchange of forests: the EUROFLUX methodology. In: Fitter, A.H., Raffaelli, D.G. (Eds.), Advances in Ecological Research. vol. 30, Academic Press, pp. 113–175. http://dx.doi.org/10.1016/S0065-2504(08)60018-5.
- Aubinet, M., Papale, D., Vesala, T. (Eds.), 2012. Eddy covariance: A practical guide to measurement and data analysis, first ed. In: Springer Atmospheric Sciences, Springer, Dordrecht, http://dx.doi.org/10.1007/978-94-007-2351-1.
- Baldocchi, D.D., 2003. Assessing the eddy covariance technique for evaluating carbon dioxide exchange rates of ecosystems: Past, present and future. Global Change Biol. 9 (4), 479–492. http://dx.doi.org/10.1046/j.1365-2486.2003.00629.x.
- Baldocchi, D.D., 2020. How eddy covariance flux measurements have contributed to our understanding of global change biology. Global Change Biol. 26 (1), 242–260. http://dx.doi.org/10.1111/gcb.14807.
- Belcher, S.E., Harman, I.N., Finnigan, J.J., 2012. The wind in the willows: flows in forest canopies in complex terrain. Annu. Rev. Fluid Mech. 44 (Volume 44, 2012), 479–504. http://dx.doi.org/10.1146/annurev-fluid-120710-101036.
- Bendix, M., Tornbjerg, T., Brix, H., 1994. Internal gas transport in typha latifolia L. and typha angustifolia L. 1. humidity-induced pressurization and convective throughflow. Aquat. Botany 49 (2), 75–89. http://dx.doi.org/10.1016/0304-3770(94)90030-2.
- Bhullar, G.S., Edwards, P.J., Venterink, H.O., 2014. Influence of different plant species on methane emissions from soil in a restored swiss wetland. PLoS One 9 (2), e89588. http://dx.doi.org/10.1371/journal.pone.0089588.
- Bonn, A., Allott, T., Evans, M., Joosten, H., Stoneman, R. (Eds.), 2016. Peatland restoration and ecosystem services: science, policy and practice. In: Ecological Reviews, Cambridge University Press, Cambridge, http://dx.doi.org/10.1017/ CBO9781139177788.
- Boonman, J., Hefting, M.M., van Huissteden, C.J.A., van den Berg, M., van Huissteden, J., Erkens, G., Melman, R., van der Velde, Y., 2021. Cutting peatland CO_2 emissions with rewetting measures. Biogeosci. Discuss. 1–31. http://dx.doi.org/10. 5194/bg-2021-276.
- Breiman, L., 2001. Random forests. Mach. Learn. 45 (1), 5–32. http://dx.doi.org/10. 1023/A:1010933404324.
- Burba, G., Anderson, T., Komissarov, A., 2019. Accounting for spectroscopic effects in laser-based open-path eddy covariance flux measurements. Global Change Biol. 25 (6), 2189–2202. http://dx.doi.org/10.1111/gcb.14614.
- Chu, H., Luo, X., Ouyang, Z., Chan, W.S., Dengel, S., Biraud, S.C., Torn, M.S., Metzger, S., Kumar, J., Arain, M.A., Arkebauer, T.J., Baldocchi, D., Bernacchi, C., Billesbach, D., Black, T.A., Blanken, P.D., Bohrer, G., Bracho, R., Brown, S., Brunsell, N.A., Chen, J., Chen, X., Clark, K., Desai, A.R., Duman, T., Durden, D., Fares, S., Forbrich, I., Gamon, J.A., Gough, C.M., Griffis, T., Helbig, M., Hollinger, D., Humphreys, E., Ikawa, H., Iwata, H., Ju, Y., Knowles, J.F., Knox, S.H., Kobayashi, H., Kolb, T., Law, B., Lee, X., Litvak, M., Liu, H., Munger, J.W., Noormets, A., Novick, K., Oberbauer, S.F., Oechel, W., Oikawa, P., Papuga, S.A., Pendall, E., Prajapati, P., Prueger, J., Quinton, W.L., Richardson, A.D., Russell, E.S., Scott, R.L., Starr, G., Staebler, R., Stoy, P.C., Stuart-Haëntjens, E., Sonnentag, O.,

- Sullivan, R.C., Suyker, A., Ueyama, M., Vargas, R., Wood, J.D., Zona, D., 2021. Representativeness of eddy-covariance flux footprints for areas surrounding Ameri-Flux sites. Agricult. Forest. Meterol. 301–302, 108350. http://dx.doi.org/10.1016/iagrfcrmpt 2021.108350
- de Jong, M., van Hal, O., Pijlman, J., van Eekeren, N., Junginger, M., 2021. Paludiculture as paludifuture on Dutch peatlands: An environmental and economic analysis of typha cultivation and insulation production. Sci. Total Environ. 792, 148161. http://dx.doi.org/10.1016/j.scitotenv.2021.148161.
- Dinsmore, K.J., Billett, M.F., Skiba, U.M., Rees, R.M., Drewer, J., Helfter, C., 2010. Role of the aquatic pathway in the carbon and greenhouse gas budgets of a peatland catchment. Global Change Biol. 16 (10), 2750–2762. http://dx.doi.org/10.1111/j. 1365-2486.2009.02119.x.
- Erkens, G., van der Meulen, M.J., Middelkoop, H., 2016. Double trouble: Subsidence and CO2 respiration due to 1,000 years of Dutch coastal peatlands cultivation. Hydrogeol. J. 24 (3), 551–568. http://dx.doi.org/10.1007/s10040-016-1380-4.
- Evans, C.D., Peacock, M., Baird, A.J., Artz, R.R.E., Burden, A., Callaghan, N., Chapman, P.J., Cooper, H.M., Coyle, M., Craig, E., Cumming, A., Dixon, S., Gauci, V., Grayson, R.P., Helfter, C., Heppell, C.M., Holden, J., Jones, D.L., Kaduk, J., Levy, P., Matthews, R., McNamara, N.P., Misselbrook, T., Oakley, S., Page, S.E., Rayment, M., Ridley, L.M., Stanley, K.M., Williamson, J.L., Worrall, F., Morrison, R., 2021. Overriding water table control on managed peatland greenhouse gas emissions. Nature 593 (7860), 548–552. http://dx.doi.org/10.1038/s41586-021-03523-1.
- Falge, E., Baldocchi, D., Olson, R., Anthoni, P., Aubinet, M., Bernhofer, C., Burba, G., Ceulemans, R., Clement, R., Dolman, H., Granier, A., Gross, P., Grünwald, T., Hollinger, D., Jensen, N.-O., Katul, G., Keronen, P., Kowalski, A., Lai, C.T., Law, B.E., Meyers, T., Moncrieff, J., Moors, E., Munger, J.W., Pilegaard, K., Rannik, Ü., Rebmann, C., Suyker, A., Tenhunen, J., Tu, K., Verma, S., Vesala, T., Wilson, K., Wofsy, S., 2001. Gap filling strategies for defensible annual sums of net ecosystem exchange. Agricult. Forest. Meterol. 107 (1), 43–69. http://dx.doi.org/10.1016/S0168-1923(00)00225-2.
- Franz, D., Koebsch, F., Larmanou, E., Augustin, J., Sachs, T., 2016. High net $\rm CO_2$ and $\rm CH_4$ release at a eutrophic shallow lake on a formerly drained fen. Biogeosciences 13 (10), 3051–3070. http://dx.doi.org/10.5194/bg-13-3051-2016.
- Frolking, S., Talbot, J., Jones, M.C., Treat, C.C., Kauffman, J.B., Tuittila, E.-S., Roulet, N., 2011. Peatlands in the earth's 21st century climate system. Environ. Rev. 19 (NA), 371–396. http://dx.doi.org/10.1139/a11-014.
- Fuchs, K., Hörtnagl, L., Buchmann, N., Eugster, W., Snow, V., Merbold, L., 2018. Management matters: Testing a mitigation strategy for nitrous oxide emissions using legumes on intensively managed grassland. Biogeosciences 15 (18), 5519–5543. http://dx.doi.org/10.5194/bg-15-5519-2018.
- Georgiev, G., Theuerkorn, W., Krus, M., Kilian, R., Grosskinsky, T., 2013. The potential role of cattail-reinforced clay plaster in sustainable building. Mires Peat 13.
- Geurts, J.J.M., van Duinen, G.J.A., van Belle, J., Whichmann, S., Wichtmann, W., Fritz, C., 2019. Recognize the high potential of paludiculture on rewetted peat soils to mitigate climate change. J. Sustain. Organic Agric. Syst. 69 (1), 5–8. http://dx.doi.org/10.3220/LBF1576769203000.
- Goodrich, J.P., Wall, A.M., Campbell, D.I., Fletcher, D., Wecking, A.R., Schipper, L.A., 2021. Improved gap filling approach and uncertainty estimation for eddy covariance N2O fluxes. Agricult. Forest. Meterol. 297, 108280. http://dx.doi.org/10. 1016/j.agrformet.2020.108280.
- Günther, A., Barthelmes, A., Huth, V., Joosten, H., Jurasinski, G., Koebsch, F., Couwenberg, J., 2020. Prompt rewetting of drained peatlands reduces climate warming despite methane emissions. Nature Commun. 11 (1), 1644. http://dx.doi. org/10.1038/s41467-020-15499-z.
- Günther, A., Huth, V., Jurasinski, G., Glatzel, S., 2015. The effect of biomass harvesting on greenhouse gas emissions from a rewetted temperate fen. GCB Bioenergy 7 (5), 1092–1106. http://dx.doi.org/10.1111/gcbb.12214.
- Hartig, F., Minunno, F., Paul, S., 2019. Bayesiantools: general-purpose MCMC and SMC samplers and tools for Bayesian statistics.
- Hendriks, D.M.D., van Huissteden, J., Dolman, A.J., 2010. Multi-technique assessment of spatial and temporal variability of methane fluxes in a peat meadow. Special Issue on Eddy Covariance (EC)Flux Measurements of Ch4 and N2O, Agricult. Forest. Meterol. Special Issue on Eddy Covariance (EC)Flux Measurements of Ch4 and N2O, 150 (6), 757–774.http://dx.doi.org/10.1016/j.agrformet.2009.06.017,
- Hendriks, L., Weideveld, S., Fritz, C., Stepina, T., Aben, R.C.H., Fung, N.E., Kosten, S., 2024. Drainage ditches are year-round greenhouse gas hotlines in temperate peat landscapes. Freshwater Biol. 69 (1), 143–156. http://dx.doi.org/10.1111/fwb. 14200.
- Huang, J., Cassiani, M., Albertson, J.D., 2011. Coherent turbulent structures across a vegetation discontinuity. Bound.-Layer Meteorol. 140 (1), 1–22. http://dx.doi.org/ 10.1007/s10546-011-9600-x.
- IPCC, 2014. In: Hiraishi, T., Krug, T., Tanabe, K., Srivastava, N., Baasansuren, J., Fukuda, M., Troxler, T. (Eds.), 2013 Supplement to the 2006 Inter-Governmental Panel on Climate Change Guidelines for National Greenhouse Gas Inventories: Wetlands. IPCC, Switzerland.
- IPCC, 2021. Climate Change 2021: The Physical Science Basis. Contribution of Working Group I to the Sixth Assessment Report of the Intergovernmental Panel on Climate Change. Cambridge University Press, Cambridge, United Kingdom and New York, NY, USA, http://dx.doi.org/10.1017/9781009157896, in press,

- Irvin, J., Zhou, S., McNicol, G., Lu, F., Liu, V., Fluet-Chouinard, E., Ouyang, Z., Knox, S.H., Lucas-Moffat, A., Trotta, C., Papale, D., Vitale, D., Mammarella, I., Alekseychik, P., Aurela, M., Avati, A., Baldocchi, D., Bansal, S., Bohrer, G., Campbell, D.I., Chen, J., Chu, H., Dalmagro, H.J., Delwiche, K.B., Desai, A.R., Euskirchen, E., Feron, S., Goeckede, M., Heimann, M., Helbig, M., Helfter, C., Hemes, K.S., Hirano, T., Iwata, H., Jurasinski, G., Kalhori, A., Kondrich, A., Lai, D.Y., Lohila, A., Malhotra, A., Merbold, L., Mitra, B., Ng, A., Nilsson, M.B., Noormets, A., Peichl, M., Rey-Sanchez, A.C., Richardson, A.D., Runkle, B.R., Schäfer, K.V., Sonnentag, O., Stuart-Haëntjens, E., Sturtevant, C., Ueyama, M., Valach, A.C., Vargas, R., Vourlitis, G.L., Ward, E.J., Wong, G.X., Zona, D., Alberto, M.C.R., Billesbach, D.P., Celis, G., Dolman, H., Friborg, T., Fuchs, K., Gogo, S., Gondwe, M.J., Goodrich, J.P., Gottschalk, P., Hörtnagl, L., Jacotot. A., Koebsch, F., Kasak, K., Maier, R., Morin, T.H., Nemitz, E., Oechel, W.C., Oikawa, P.Y., Ono, K., Sachs, T., Sakabe, A., Schuur, E.A., Shortt, R., Sullivan, R.C., Szutu, D.J., Tuittila, E.-S., Varlagin, A., Verfaillie, J.G., Wille, C., Windham-Myers, L., Poulter, B., Jackson, R.B., 2021. Gap-filling eddy covariance methane fluxes: comparison of machine learning model predictions and uncertainties at FLUXNET-CH4 wetlands. Agricult. Forest. Meterol. 308-309, 108528. http://dx. doi.org/10.1016/j.agrformet.2021.108528.
- Joosten, H., Sirin, A., Couwenberg, J., Laine, J., Smith, P., 2016. The role of peatlands in climate regulation. In: Bonn, A., Joosten, H., Evans, M., Stoneman, R., Allott, T. (Eds.), Peatland Restoration and Ecosystem Services: Science, Policy and Practice. In: Ecological Reviews, Cambridge University Press, Cambridge, pp. 63–76. http://dx.doi.org/10.1017/CBO9781139177788.005.
- Joosten, H., Tapio-Biström, M.L., Tol, S., 2012. Peatlands: Guidance for Climate Change Mitigation through Conservation, Rehabilitation and Sustainable Use. Food and Agriculture Organization of the United Nations.
- Kanani-Sühring, F., Raasch, S., 2015. Spatial variability of scalar concentrations and fluxes downstream of a clearing-to-forest transition: A large-eddy simulation study. Bound.-Layer Meteorol. 155 (1), 1–27. http://dx.doi.org/10.1007/s10546-014-9986-3
- Kim, J., Hwang, T., Schaaf, C.L., Kljun, N., Munger, J.W., 2018. Seasonal variation of source contributions to eddy-covariance CO2 measurements in a mixed hardwoodconifer forest. Agricult. Forest. Meterol. 253–254, 71–83. http://dx.doi.org/10. 1016/j.agrformet.2018.02.004.
- Kim, Y., Johnson, M.S., Knox, S.H., Black, T.A., Dalmagro, H.J., Kang, M., Kim, J., Baldocchi, D., 2020. Gap-filling approaches for eddy covariance methane fluxes: A comparison of three machine learning algorithms and a traditional method with principal component analysis. Global Change Biol. 26 (3), 1499–1518. http: //dx.doi.org/10.1111/gcb.14845.
- Kivimäki, S.K., Yli-Petäys, M., Tuittila, E.-S., 2008. Carbon sink function of sedge and sphagnum patches in a restored cut-away peatland: increased functional diversity leads to higher production. J. Appl. Ecol. 45 (3), 921–929. http://dx.doi.org/10. 1111/j.1365-2664.2008.01458.x, arXiv:20144046.
- Klaassen, W., Sogachev, A., 2006. Flux footprint simulation downwind of a forest edge. Bound.-Layer Meteorol. 121 (3), 459–473. http://dx.doi.org/10.1007/s10546-006-9078-0.
- Kljun, N., Calanca, P., Rotach, M.W., Schmid, H.P., 2015. A simple two-dimensional parameterisation for flux footprint prediction (FFP). Geosci. Model Dev. 8 (11), 3695–3713. http://dx.doi.org/10.5194/gmd-8-3695-2015.
- Kljun, N., Rotach, M., Schmid, H., 2002. A three-dimensional backward Lagrangian footprint model for a wide range of boundary-layer stratifications. Bound.-Layer Meteorol. 103 (2), 205–226. http://dx.doi.org/10.1023/A:1014556300021.
- Knox, S.H., Jackson, R.B., Poulter, B., McNicol, G., Fluet-Chouinard, E., Zhang, Z., Hugelius, G., Bousquet, P., Canadell, J.G., Saunois, M., Papale, D., Chu, H., Keenan, T.F., Baldocchi, D., Torn, M.S., Mammarella, I., Trotta, C., Aurela, M., Bohrer, G., Campbell, D.I., Cescatti, A., Chamberlain, S., Chen, J., Chen, W., Dengel, S., Desai, A.R., Euskirchen, E., Friborg, T., Gasbarra, D., Goded, I., Goeckede, M., Heimann, M., Helbig, M., Hirano, T., Hollinger, D.Y., Iwata, H., Kang, M., Klatt, J., Krauss, K.W., Kutzbach, L., Lohila, A., Mitra, B., Morin, T.H., Nilsson, M.B., Niu, S., Noormets, A., Oechel, W.C., Peichl, M., Peltola, O., Reba, M.L., Richardson, A.D., Runkle, B.R.K., Ryu, Y., Sachs, T., Schäfer, K.V.R., Schmid, H.P., Shurpali, N., Sonnentag, O., Tang, A.C.I., Ueyama, M., Vargas, R., Vesala, T., Ward, E.J., Windham-Myers, L., Wohlfahrt, G., Zona, D., 2019. FLUXNET-CH4 synthesis activity: objectives, observations, and future directions. Bull. Am. Meteorol. Soc. 100 (12), 2607–2632. http://dx.doi.org/10.1175/BAMS-D-18-0268.1.
- Knox, S.H., Sturtevant, C., Matthes, J.H., Koteen, L., Verfaillie, J., Baldocchi, D., 2015. Agricultural peatland restoration: Effects of land-use change on greenhouse gas (CO2 and CH4) fluxes in the sacramento-san Joaquin Delta. Global Change Biol. 21 (2), 750–765. http://dx.doi.org/10.1111/gcb.12745.
- Koehler, A.K., Sottocornola, M., Kiely, G., 2011. How strong is the current carbon sequestration of an atlantic blanket bog? Global Change Biol. 17 (1), 309–319. http://dx.doi.org/10.1111/j.1365-2486.2010.02180.x.
- Kormann, R., Meixner, F.X., 2001. An analytical footprint model for non-neutral stratification. Bound.-Layer Meteorol. 99 (2), 207–224. http://dx.doi.org/10.1023/ A:1018991015119.
- Krus, M., Werner, T., Großkinsky, T., Georgiev, G., 2015. A new load-bearing insulation material made of cattail. Acad. J. Civ. Eng. 33 (2), 666–673. http://dx.doi.org/10. 26168/icbbm2015.104.

- Lahtinen, L., Mattila, T., Myllyviita, T., Seppälä, J., Vasander, H., 2022. Effects of paludiculture products on reducing greenhouse gas emissions from agricultural peatlands. Ecol. Eng. 175, 106502. http://dx.doi.org/10.1016/j.ecoleng.2021. 106502.
- Lamers, L.P.M., Vile, M.A., Grootjans, A.P., Acreman, M.C., van Diggelen, R., Evans, M.G., Richardson, C.J., Rochefort, L., Kooijman, A.M., Roelofs, J.G.M., Smolders, A.J.P., 2015. Ecological restoration of rich fens in Europe and North America: From trial and error to an evidence-based approach. Biol. Rev. 90 (1), 182–203. http://dx.doi.org/10.1111/brv.12102.
- Langeveld, C.A., Segers, R., Dirks, B.O.M., van den Pol-van Dasselaar, A., Velthof, G.L., Hensen, A., 1997. Emissions of CO2, CH4 and N2O from pasture on drained peat soils in the Netherlands. Eur. J. Agron. 7 (1), 35–42. http://dx.doi.org/10.1016/ \$1161-0301(97)00036-1.
- Lasslop, G., Reichstein, M., Papale, D., Richardson, A.D., Arneth, A., Barr, A., Stoy, P., Wohlfahrt, G., 2010. Separation of net ecosystem exchange into assimilation and respiration using a light response curve approach: Critical issues and global evaluation. Global Change Biol. 16 (1), 187–208. http://dx.doi.org/10.1111/j. 1365-2486.2009.02041.x.
- Leclerc, M.Y., Foken, T., 2014. Footprints in Micrometeorology and Ecology. Springer, Heidelberg.
- Leifeld, J., Menichetti, L., 2018. The underappreciated potential of peatlands in global climate change mitigation strategies. Nature Commun. 9 (1), 1071. http://dx.doi. org/10.1038/s41467-018-03406-6.
- Leifeld, J., Wüst-Galley, C., Page, S., 2019. Intact and managed peatland soils as a source and sink of GHGs from 1850 to 2100. Nature Clim. Change 9 (12), 945–947. http://dx.doi.org/10.1038/s41558-019-0615-5.
- Levy, P.E., Burden, A., Cooper, M.D.A., Dinsmore, K.J., Drewer, J., Evans, C., Fowler, D., Gaiawyn, J., Gray, A., Jones, S.K., Jones, T., McNamara, N.P., Mills, R., Ostle, N., Sheppard, L.J., Skiba, U., Sowerby, A., Ward, S.E., Zieliński, P., 2012. Methane emissions from soils: Synthesis and analysis of a large UK data set. Global Change Biol. 18 (5), 1657–1669. http://dx.doi.org/10.1111/j.1365-2486.2011.02616.x.
- Lloyd, J., Taylor, J.A., 1994. On the temperature dependence of soil respiration. Funct. Ecol. 8 (3), 315–323. http://dx.doi.org/10.2307/2389824, arXiv:2389824.
- Luamkanchanaphan, T., Chotikaprakhan, S., Jarusombati, S., 2012. A study of physical, mechanical and thermal properties for thermal insulation from narrow-leaved cattail fibers. APCBEE Procedia 1, 46–52. http://dx.doi.org/10.1016/j.apcbee.2012. 03.009.
- Mauder, M., Cuntz, M., Drüe, C., Graf, A., Rebmann, C., Schmid, H.P., Schmidt, M., Steinbrecher, R., 2013. A strategy for quality and uncertainty assessment of longterm eddy-covariance measurements. Agricult. Forest. Meterol. 169, 122–135. http: //dx.doi.org/10.1016/j.agrformet.2012.09.006.
- Mauder, M., Foken, T., 2004. Documentation and instruction manual of the eddy covariance software package TK2. In: Arbeitsergebnisse, Vol 26, Universität Bayreuth, Abteilung Mikrometeorologie, Bayreuth.
- Mauder, M., Foken, T., Aubinet, M., Ibrom, A., 2021. Eddy-covariance measurements.
 In: Foken, T. (Ed.), Springer Handbook of Atmospheric Measurements. Springer International Publishing, Cham, pp. 1473–1504. http://dx.doi.org/10.1007/978-3-030-52171-455
- McDermitt, D., Burba, G., Xu, L., Anderson, T., Komissarov, A., Riensche, B., Schedlbauer, J., Starr, G., Zona, D., Oechel, W., Oberbauer, S., Hastings, S., 2011. A new low-power, open-path instrument for measuring methane flux by eddy covariance. Appl. Phys. B 102 (2), 391–405. http://dx.doi.org/10.1007/s00340-010-4307-0.
- Minke, M., Augustin, J., Burlo, A., Yarmashuk, T., Chuvashova, H., Thiele, A., Freibauer, A., Tikhonov, V., Hoffmann, M., 2016. Water level, vegetation composition, and plant productivity explain greenhouse gas fluxes in temperate cutover fens after inundation. Biogeosciences 13 (13), 3945–3970. http://dx.doi.org/10.5194/bg-13-3945-2016.
- Moncrieff, J., Clement, R., Finnigan, J., Meyers, T., 2004. Averaging, detrending, and filtering of eddy covariance time series. In: Lee, X., Massman, W., Law, B. (Eds.), Handbook of Micrometeorology: a Guide for Surface Flux Measurement and Analysis. In: Atmospheric and Oceanographic Sciences Library, Springer Netherlands, Dordrecht, pp. 7–31. http://dx.doi.org/10.1007/1-4020-2265-4_2.
- Moncrieff, J.B., Massheder, J.M., de Bruin, H., Elbers, J., Friborg, T., Heusinkveld, B., Kabat, P., Scott, S., Soegaard, H., Verhoef, A., 1997. A system to measure surface fluxes of momentum, sensible heat, water vapour and carbon dioxide. HAPEX-Sahel, J. Hydrol. HAPEX-Sahel, 188–189, 589–611.http://dx.doi.org/10.1016/S0022-1694(96)03194-0.
- Nilsson, M., Sagerfors, J., Buffam, I., Laudon, H., Eriksson, T., Grelle, A., Klemedtsson, L., Weslien, P., Lindroth, A., 2008. Contemporary carbon accumulation in a boreal oligotrophic minerogenic mire a significant sink after accounting for all C-fluxes. Global Change Biol. 14 (10), 2317–2332. http://dx.doi.org/10.1111/j.1365-2486.2008.01654.x.
- Papale, D., Reichstein, M., Aubinet, M., Canfora, E., Bernhofer, C., Kutsch, W., Longdoz, B., Rambal, S., Valentini, R., Vesala, T., Yakir, D., 2006. Towards a standardized processing of net ecosystem exchange measured with eddy covariance technique: Algorithms and uncertainty estimation. Biogeosciences 3 (4), 571–583. http://dx.doi.org/10.5194/bg-3-571-2006.
- Peacock, M., Audet, J., Bastviken, D., Futter, M.N., Gauci, V., Grinham, A., Harrison, J.A., Kent, M.S., Kosten, S., Lovelock, C.E., Veraart, A.J., Evans, C.D., 2021. Global importance of methane emissions from drainage ditches and canals. Environ. Res. Lett. 16 (4), 044010. http://dx.doi.org/10.1088/1748-9326/abeb36.

- Pijlman, J., Geurts, J., Vroom, R., Bestman, M., Fritz, C., van Eekeren, N., 2019. The effects of harvest date and frequency on the yield, nutritional value and mineral content of the paludiculture crop cattail (typha latifolia L.) in the first year after planting. Mires Peat 25 (4), 1–19.
- Poyda, A., Reinsch, T., Skinner, R.H., Kluß, C., Loges, R., Taube, F., 2017. Comparing chamber and eddy covariance based net ecosystem CO2 exchange of fen soils. J. Plant Nutr. Soil Sci. 180 (2), 252–266. http://dx.doi.org/10.1002/jpln.201600447.
- Prananto, J.A., Minasny, B., Comeau, L.-P., Rudiyanto, R., Grace, P., 2020. Drainage increases CO2 and N2O emissions from tropical peat soils. Global Change Biol. 26 (8), 4583–4600. http://dx.doi.org/10.1111/gcb.15147.
- R Core Team, 2022. R: A Language and Environment for Statistical Computing. R Foundation for Statistical Computing, Vienna, Austria.
- Reichstein, M., Falge, E., Baldocchi, D., Papale, D., Aubinet, M., Berbigier, P., Bernhofer, C., Buchmann, N., Gilmanov, T., Granier, A., Grünwald, T., Havránková, K., Ilvesniemi, H., Janous, D., Knohl, A., Laurila, T., Lohila, A., Loustau, D., Matteucci, G., Meyers, T., Miglietta, F., Ourcival, J.M., Pumpanen, J., Rambal, S., Rotenberg, E., Sanz, M., Tenhunen, J., Seufert, G., Vaccari, F., Vesala, T., Yakir, D., Valentini, R., 2005. On the separation of net ecosystem exchange into assimilation and ecosystem respiration: Review and improved algorithm. Global Change Biol. 11 (9), 1424–1439. http://dx.doi.org/10.1111/j.1365-2486.2005.001002.x.
- Renou-Wilson, F., Barry, C., Müller, C., Wilson, D., 2014. The impacts of drainage, nutrient status and management practice on the full carbon balance of grasslands on organic soils in a maritime temperate zone. Biogeosciences 11 (16), 4361–4379. http://dx.doi.org/10.5194/bg-11-4361-2014.
- Rey-Sanchez, C., Arias-Ortiz, A., Kasak, K., Chu, H., Szutu, D., Verfaillie, J., Baldocchi, D., 2022. Detecting hot spots of methane flux using footprint-weighted flux maps. J. Geophys. Res.: Biogeosci. 127 (8), http://dx.doi.org/10.1029/2022JG006977. e2022JG006977.
- Riederer, M., Serafimovich, A., Foken, T., 2014. Net ecosystem CO₂ exchange measurements by the closed chamber method and the eddy covariance technique and their dependence on atmospheric conditions. Atmos. Meas. Tech. 7 (4), 1057–1064. http://dx.doi.org/10.5194/amt-7-1057-2014.
- Rinne, J., Riutta, T., Pihlatie, M., Aurela, M., Haapanala, S., Tuovinen, J.P., Tuittila, E.S., Vesala, T., 2007. Annual cycle of methane emission from a boreal fen measured by the eddy covariance technique. Tellus B: Chem. Phys. Meteorol. 59 (3), 449–457. http://dx.doi.org/10.1111/j.1600-0889.2007.00261.x.
- Rocha, A.V., Goulden, M.L., 2009. Why is marsh productivity so high? new insights from eddy covariance and biomass measurements in a typha marsh. Agricult. Forest. Meterol. 149 (1), 159–168. http://dx.doi.org/10.1016/j.agrformet.2008.07.010.
- Schrier-Uijl, A.P., Kroon, P.S., Hendriks, D.M.D., Hensen, A., Van Huissteden, J., Berendse, F., Veenendaal, E.M., 2014. Agricultural peatlands: Towards a greenhouse gas sink a synthesis of a Dutch landscape study. Biogeosciences 11 (16), 4559–4576. http://dx.doi.org/10.5194/bg-11-4559-2014.
- Schrier-Uijl, A.P., Kroon, P.S., Leffelaar, P.A., van Huissteden, J.C., Berendse, F., Veenendaal, E.M., 2010. Methane emissions in two drained peat agro-ecosystems with high and low agricultural intensity. Plant Soil 329 (1), 509–520. http://dx.doi.org/10.1007/s11104-009-0180-1.
- Schrier-Uijl, A.P., Veraart, A.J., Leffelaar, P.A., Berendse, F., Veenendaal, E.M., 2011. Release of CO2 and CH4 from lakes and drainage ditches in temperate wetlands. Biogeochemistry 102 (1), 265–279. http://dx.doi.org/10.1007/s10533-010-9440-7.
- Schwieger, S., Kreyling, J., Couwenberg, J., Smiljanić, M., Weigel, R., Wilmking, M., Blume-Werry, G., 2021. Wetter is better: rewetting of minerotrophic peatlands increases plant production and moves them towards carbon sinks in a dry year. Ecosystems 24 (5), 1093–1109. http://dx.doi.org/10.1007/s10021-020-00570-z.
- Sogachev, A., Leclerc, M.Y., Zhang, G., Rannik, Ü., Vesala, T., 2008. Co2 fluxes near a forest edge: A numerical study. Ecol. Appl. 18 (6), 1454–1469. http://dx.doi.org/10.1890/06-1119.1.
- Staudhammer, C.L., Malone, S.L., Zhao, J., Yu, Z., Starr, G., Oberbauer, S.F., 2022. Methane emissions from subtropical wetlands: An evaluation of the role of data filtering on annual methane budgets. Agricult. Forest. Meterol. 321, 108972. http://dx.doi.org/10.1016/j.agrformet.2022.108972.
- ter Braak, C.J.F., Vrugt, J.A., 2008. Differential evolution Markov chain with snooker updater and fewer chains. Stat. Comput. 18 (4), 435–446. http://dx.doi.org/10. 1007/s11222-008-9104-9.
- Tiemeyer, B., Albiac Borraz, E., Augustin, J., Bechtold, M., Beetz, S., Beyer, C., Drösler, M., Ebli, M., Eickenscheidt, T., Fiedler, S., Förster, C., Freibauer, A., Giebels, M., Glatzel, S., Heinichen, J., Hoffmann, M., Höper, H., Jurasinski, G., Leiber-Sauheitl, K., Peichl-Brak, M., Roßkopf, N., Sommer, M., Zeitz, J., 2016. High emissions of greenhouse gases from grasslands on peat and other organic soils. Global Change Biol. 22 (12), 4134–4149. http://dx.doi.org/10.1111/gcb.13303.
- Tuovinen, J.P., Aurela, M., Hatakka, J., Räsänen, A., Virtanen, T., Mikola, J., Ivakhov, V., Kondratyev, V., Laurila, T., 2019. Interpreting eddy covariance data from heterogeneous Siberian tundra: Land-cover-specific methane fluxes and spatial representativeness. Biogeosciences 16 (2), 255–274. http://dx.doi.org/10.5194/bg-16-255-2019.
- Turetsky, M.R., Kotowska, A., Bubier, J., Dise, N.B., Crill, P., Hornibrook, E.R.C., Minkkinen, K., Moore, T.R., Myers-Smith, I.H., Nykänen, H., Olefeldt, D., Rinne, J., Saarnio, S., Shurpali, N., Tuittila, E.S., Waddington, J.M., White, J.R., Wickland, K.P., Wilmking, M., 2014. A synthesis of methane emissions from 71 northern, temperate, and subtropical wetlands. Global Change Biol. 20 (7), 2183–2197. http://dx.doi.org/10.1111/gcb.12580.

- van den Berg, M., Gremmen, T.M., Vroom, R.J.E., van Huissteden, J., Boonman, J., van Huissteden, C.J.A., van der Velde, Y., Smolders, A.J.P., van de Riet, B.P., 2024. A case study on topsoil removal and rewetting for paludiculture: Effect on biogeochemistry and greenhouse gas emissions from *Typha Latifolia*, *Typha Angustifolia*, and *Azolla Filiculoides*. Biogeosciences 21 (11), 2669–2690. http://dx.doi.org/10.5194/bg-21-2669-2024.
- van den Berg, M., Ingwersen, J., Lamers, M., Streck, T., 2016. The role of *Phragmites* in the CH₄ and CO₂ fluxes in a minerotrophic peatland in southwest Germany. Biogeosciences 13 (21), 6107–6119. http://dx.doi.org/10.5194/bg-13-6107-2016.
- van den Berg, M., van den Elzen, E., Ingwersen, J., Kosten, S., Lamers, L.P.M., Streck, T., 2020. Contribution of plant-induced pressurized flow to CH₄ emission from a phragmites fen. Sci. Rep. 10 (1), 12304. http://dx.doi.org/10.1038/s41598-020-69034-7
- Vesala, T., Kljun, N., Rannik, Ü., Rinne, J., Sogachev, A., Markkanen, T., Sabelfeld, K., Foken, T., Leclerc, M.Y., 2008. Flux and concentration footprint modelling: state of the art. Environ. Pollut. 152 (3), 653–666. http://dx.doi.org/10.1016/j.envpol. 2007.06.070.
- Vickers, D., Mahrt, L., 1997. Quality control and flux sampling problems for tower and aircraft data. J. Atmos. Ocean. Technol. 14 (3), 512–526. http://dx.doi.org/ 10.1175/1520-0426(1997)014<0512:QCAFSP>2.0.CO;2.
- Vroom, R.J.E., van den Berg, M., Pangala, S.R., van der Scheer, O.E., Sorrell, B.K., 2022. Physiological processes affecting methane transport by wetland vegetation A review. Aquat. Botany 182, 103547. http://dx.doi.org/10.1016/j.aquabot.2022. 103547.
- Waddington, J.M., Strack, M., Greenwood, M.J., 2010. Toward restoring the net carbon sink function of degraded peatlands: short-term response in CO2 exchange to ecosystem-scale restoration. J. Geophys. Res.: Biogeosci. 115 (G1), http://dx.doi. org/10.1029/2009JG001090.
- Wall, A.M., Campbell, D.I., Mudge, P.L., Schipper, L.A., 2020. Temperate grazed grassland carbon balances for two adjacent paddocks determined separately from one eddy covariance system. Agricult. Forest. Meterol. 287, 107942. http://dx.doi. org/10.1016/j.agrformet.2020.107942.
- Wang, W., Davis, K.J., Cook, B.D., Butler, M.P., Ricciuto, D.M., 2006. Decomposing CO2 fluxes measured over a mixed ecosystem at a tall tower and extending to a region: A case study. J. Geophys. Res.: Biogeosci. 111 (G2), http://dx.doi.org/10. 1029/2005.IG000093
- Webb, E.K., Pearman, G.I., Leuning, R., 1980. Correction of flux measurements for density effects due to heat and water vapour transfer. Q. J. R. Meteorol. Soc. 106 (447), 85–100. http://dx.doi.org/10.1002/qj.49710644707.
- Weideveld, S.T.J., Liu, W., van den Berg, M., Lamers, L.P.M., Fritz, C., 2021. Conventional subsoil irrigation techniques do not lower carbon emissions from drained peat meadows. Biogeosciences 18 (12), 3881–3902. http://dx.doi.org/10.5194/bg-18-3881-2021.
- Wichtmann, W., Schröder, C., Joosten, H., 2016. Paludiculture Productive Use of Wet Peatlands. Schweizerbart'sche Verlagsbuchhandlung.
- Wickham, H., Averick, M., Bryan, J., Chang, W., McGowan, L.D., François, R., Grolemund, G., Hayes, A., Henry, L., Hester, J., Kuhn, M., Pedersen, T.L., Miller, E., Bache, S.M., Müller, K., Ooms, J., Robinson, D., Seidel, D.P., Spinu, V., Takahashi, K., Vaughan, D., Wilke, C., Woo, K., Yutani, H., 2019. Welcome to the tidyverse. J. Open Source Softw. 4 (43), 1686. http://dx.doi.org/10.21105/joss. 01686.
- Wilson, D., Alm, J., Laine, J., Byrne, K.A., Farrell, E.P., Tuittila, E.S., 2009. Rewetting of cutaway peatlands: are we re-creating hot spots of methane emissions? Restoration Ecol. 17 (6), 796–806. http://dx.doi.org/10.1111/j.1526-100X.2008.00416.x.
- Wilson, D., Dixon, S.D., Artz, R.R.E., Smith, T.E.L., Evans, C.D., Owen, H.J.F., Archer, E., Renou-Wilson, F., 2015. Derivation of greenhouse gas emission factors for peatlands managed for extraction in the Republic of Ireland and the United Kingdom. Biogeosciences 12 (18), 5291–5308. http://dx.doi.org/10.5194/bg-12-5291-2015.
- Wilson, D., Farrell, C.A., Fallon, D., Moser, G., Müller, C., Renou-Wilson, F., 2016.
 Multiyear greenhouse gas balances at a rewetted temperate peatland. Global Change Biol. 22 (12), 4080–4095. http://dx.doi.org/10.1111/gcb.13325.
- Wilson, D., Tuittila, E.S., Alm, J., Laine, J., Farrell, E.P., Byrne, K.A., 2007. Carbon dioxide dynamics of a restored maritime peatland. Ecoscience 14 (1), 71–80. http://dx.doi.org/10.2980/1195-6860(2007)14[71:CDDOAR]2.0.CO;2.
- Wohlfahrt, G., Klumpp, K., Soussana, J.F., 2012. Eddy covariance measurements over grasslands. In: Aubinet, M., Papale, D., Vesala, T. (Eds.), Eddy Covariance: A Practical Guide to Measurement and Data Analysis, first ed. In: Springer Atmospheric Sciences, Springer, Dordrecht, pp. 333–344. http://dx.doi.org/10.1007/978-94-007-2351-1.
- Wutzler, T., Lucas-Moffat, A., Migliavacca, M., Knauer, J., Sickel, K., Šigut, L., Menzer, O., Reichstein, M., 2018. Basic and extensible post-processing of eddy covariance flux data with REddyProc. Biogeosciences 15 (16), 5015–5030. http: //dx.doi.org/10.5194/bg-15-5015-2018.
- Yu, Z., Loisel, J., Brosseau, D.P., Beilman, D.W., Hunt, S.J., 2010. Global peatland dynamics since the last glacial maximum. Geophys. Res. Lett. 37 (13), http: //dx.doi.org/10.1029/2010GL043584.